IOP Publishing Physics in Medicine and Biology

Phys. Med. Biol. **58** (2013) R187–R220 doi:10.1088/0031-9155/58/17/R187

TOPICAL REVIEW

Automated segmentation of pulmonary structures in thoracic computed tomography scans: a review

Eva M van Rikxoort and Bram van Ginneken

Diagnostic Image Analysis Group, Department of Radiology, Radboud University Nijmegen Medical Centre, The Netherlands

E-mail: e.vanrikxoort@rad.umcn.nl

Received 28 March 2013, in final form 18 June 2013
Published 16 August 2013
Online at stacks.iop.org/PMB/58/R187

Abstract

Computed tomography (CT) is the modality of choice for imaging the lungs *in vivo*. Sub-millimeter isotropic images of the lungs can be obtained within seconds, allowing the detection of small lesions and detailed analysis of disease processes. The high resolution of thoracic CT and the high prevalence of lung diseases require a high degree of automation in the analysis pipeline. The automated segmentation of pulmonary structures in thoracic CT has been an important research topic for over a decade now. This systematic review provides an overview of current literature. We discuss segmentation methods for the lungs, the pulmonary vasculature, the airways, including airway tree construction and airway wall segmentation, the fissures, the lobes and the pulmonary segments. For each topic, the current state of the art is summarized, and topics for future research are identified.

(Some figures may appear in colour only in the online journal)

1. Introduction

To be able to detect and quantify abnormalities in a certain anatomical structure, such as the lungs, the first step is to localize and segment the structure of interest. Therefore, for any automated analysis of medical images, the segmentation is an important prerequisite. Computed tomography (CT) is currently the most sensitive way to image the lungs *in vivo* and therefore the modality of choice for lung imaging. Since the advent of multi-detector CT scanners, sub-millimeter isotropic scans of the thorax can be obtained in a few seconds. These isotropic CT scans allow for the analysis of small lesions and changes but their availability also increased the need for an automated analysis since each scan typically contains over 400 axial slices.

Lung diseases are highly prevalent and have a high morbidity and mortality associated with them. In the top ten causes of death worldwide in 2010 (Lozano *et al* 2012), chronic obstructive pulmonary disease (COPD) ranks no. 3, lower respiratory infections rank no. 4,

lung cancer ranks no. 5 and tuberculosis ranks no. 10. Recently, it has become apparent that low-dose CT screening can reduce lung cancer mortality (Aberle *et al* 2011), by far the most common cause of cancer death among both men and women (Jemal *et al* 2011). In addition, lung diseases such as asthma, cystic fibrosis and interstitial lung disease are often diagnosed and monitored with CT imaging.

The objective of this review is to provide an overview of the literature on the segmentation of anatomical structures in thoracic CT scans. The most important applications of automated segmentation in such scans are the localization of normal anatomy for the development of computer-aided diagnosis, detection (CAD), quantification and treatment planning. For a CAD system to be able to aid the radiologists in the detection of lesions, e.g. lung nodules, the system needs to know which part of the CT scan comprises the anatomical structure of interest in order not to indicate lesions in irrelevant areas. Radiologists are very good at recognizing diseases and qualitatively judging their severity, but exact quantitation from thoracic CT scans is challenging for humans (Kim *et al* 2013) and computers generally perform better. For example, the extent of lung emphysema, one of the manifestations of COPD, is often quantified as the percentage of lung tissue below a certain threshold on the CT scan. For humans, precisely quantifying this in 3D chest CT scans is almost impossible, whereas computers can do this rapidly and precisely provided an accurate segmentation of the lungs is available. Other commonly used quantitative measures are volume measurements. The (change in) volume of structures can provide important diagnostic information, e.g. the diameters of the airways and the airway walls are used in the diagnosis of COPD, asthma and cystic fibrosis. It is evident that in order to perform reliable volume measurements of a structure, an accurate segmentation is required.

This review will discuss algorithms for the segmentation of the lungs, vessels, airways, fissures, lobes and pulmonary segments from chest CT scans. Each section will provide an overview of common methodology, an overview of papers published so far and a discussion of the challenges ahead. The first few sections will provide background information on how the literature was collected, on pulmonary anatomy and on thoracic CT imaging. This review concludes with a general discussion on the current state of the art and the challenges ahead.

2. Literature selection

The literature for this systematic review was collected by performing the following search in the online database PubMed: `(''computed tomography'' OR CT) AND (chest OR thorax OR lung OR lungs OR pulmonary OR airways) AND (segmentation OR delineation OR extraction)`. This resulted in 925 hits. We took all papers through 2012 into account. The first paper was published in 1975, also the first year when a substantial number of papers on CT appeared. The largest number of papers, 133, was published in 2012. Figure 1 shows the steep growth of papers on the topic of this review. For reference, we have also plotted the increase in papers found in PubMed for the three substrings in our query that retrieve papers on CT, on lung and on segmentation, respectively. All these topics show an increasing trend as well, partly reflecting the general increase in numbers of papers produced by the scientific community and contained in PubMed. However, the growth in papers on 'lung' is slower than papers that mention on CT or segmentation. The growth in segmentation papers in thoracic CT is markedly stronger than any of the three subqueries. In the early 2000s, a steep increase in the number of papers is observed.

For all hits, all journal publications about the segmentation in chest CT scans which appeared in *Medical Physics*, *IEEE Transactions on Medical Imaging*, *Medical Image Analysis*, *Physics in Medicine and Biology*, *Academic Radiology*, *Radiology*, *European Radiology*, *American Journal of Roentgenology* and the *American Journal of Respiratory* and *Critical*

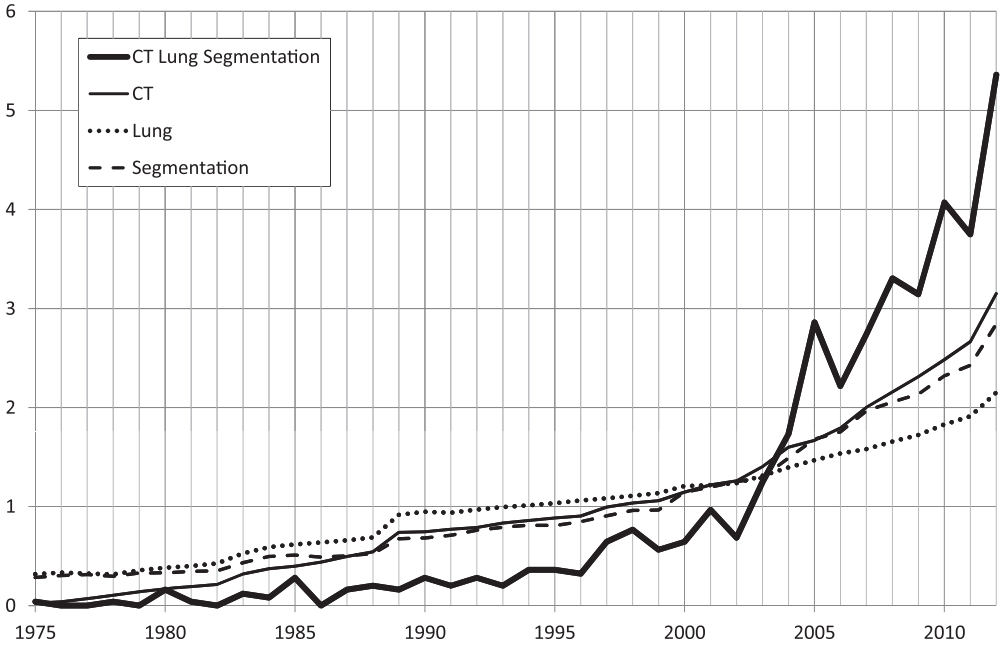

Figure 1. Illustration of the growth in the number of papers on the segmentation of pulmonary anatomy from thoracic CT scans. We used the compound search string provided in the text and plot the number of publications per year divided by the average number of publications per year in the period 1975–2012. This number was 24.8. For comparison, the same was done using the three search queries that made up the compound queries: (`''computed tomography'' OR CT`) resulted in 8031 papers per year in this period, (`chest OR thorax OR lung OR lungs OR pulmonary OR airways`) generated 19 370 hits per year on average and (`segmentation OR delineation OR extraction`) produced 4481 publications per year.

Care Medicine were inspected and taken into account if relevant. This selection formed the core of papers for this review. Papers from other journals, and conference publications from *SPIE Medical Imaging*, *Medical Image Computing and Computer Assisted Intervention*, *Information Processing in Medical Imaging* and the *IEEE Symposium on Biomedical Imaging* were added if they presented methods with different approaches compared to the core papers. References in all papers were checked and added when they presented different approaches. We used Google Scholar and IEEEXplore to search papers not listed in PubMed. In case we encountered several papers from one author group about the same subject, we generally picked the most detailed one for this review.

3. Pulmonary anatomy

This section provides basic information about the pulmonary anatomy that can be segmented from a chest CT scan. Figure 2 shows a schematic drawing of the lungs and the airway tree. In figure 3, several anatomical structures are indicated on an axial slice of a chest CT scan.

Within the thorax, the lungs are enclosed by the ribs and the base of the lungs rests on the diaphragm. The space in between the two lungs is called the mediastinum, which contains the heart, major blood vessels, the esophagus, the trachea and main bronchi, and several other thoracic structures. The airways, blood vessels and nerves enter the lungs from the mediastinum at the hilum. The lungs themselves comprise airways, vessels and a connective

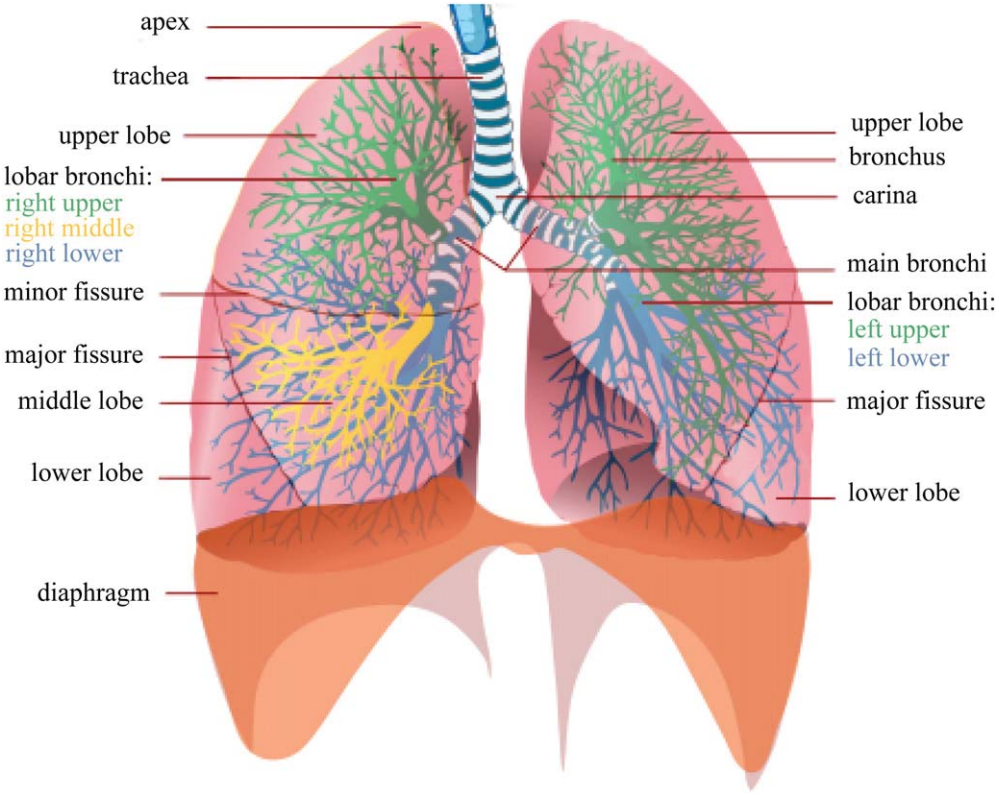

Figure 2. A schematic drawing of the lungs and airway tree in which several anatomical structures are indicated. Image adapted from Wikipedia.

tissue framework referred to as the interstitium. The gas exchange in the lungs takes place in the alveoli which are much too small to be visible on CT. The alveoli and the interstitium make up the lung parenchyma, which comprises the major part of the lungs on CT and has a density between −800 and −900 Hounsfield Units (HU), indicating that at full inspiration lung parenchyma voxels consist of about 80–90% of air.

The starting branch of the airway tree (or bronchial tree) is the trachea. The trachea divides into two main bronchi: one to the left lung and one to the right lung, at the anatomical point known as the carina. The left main bronchus subdivides into two lobar bronchi and the right main bronchus divides into three. The lobar bronchi divide into segmental bronchi, and subsequently the airway tree divides into increasingly finer branches. The airways undergo approximately 23 divisions between the trachea and the alveolar sacs, the functional units of the lung where gas exchange takes place. The airways consist of a lumen, that is filled with air, and an airway wall. On a CT scan, the lumen and wall can be separately identified and branches can be detected up to the 16th subdivision (1–2 mm) (Prokop *et al* 2003).

There are two vascular trees in the lungs: the arterial tree and the venous tree. The arterial tree supplies the lungs with blood and arteries typically run alongside the bronchi. The veins drain blood from the lungs and typically do not run along the bronchi. Arteries and veins cannot be separated by their appearance on a CT scan when no contrast material has been injected into the patient.

The lungs are subdivided into lobes. The left lung consists of two lobes, the upper and lower lobes, while the right lung has three lobes, the upper part being divided into a middle

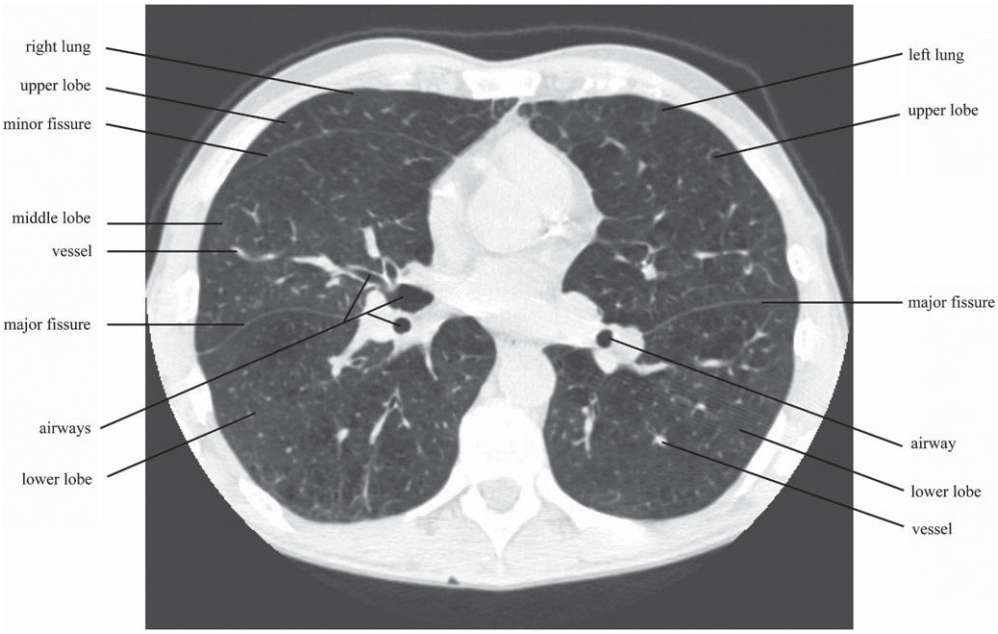

Figure 3. An axial slice of a CT scan with labeled anatomical structures.

and upper lobe. The physical boundaries between the lobes are the interlobar fissures, which consist of a double layer of visceral pleura and constitute anatomical barriers to the invasion of disease (Gülsün *et al* 2006). The fissures can be distinguished in CT scans as bright surfaces in the lungs. Each lobe has a separate supply of air by the lobar bronchi; similarly, each lobe has a separate vascular, nerve and lymphatic supplies which allows the lobes to function relatively independent of each other. If the interlobar fissures do not completely delineate the lobar boundary, which is often the case (Raasch *et al* 1982, Hayashi *et al* 2001, Aziz *et al* 2004, Gülsün *et al* 2006), the different lobes are connected and might not function independently.

The lobes are further subdivided into segments. Unlike the lobes, the segments are almost never separated by fissures, but by thin membranes of connective tissue. This tissue cannot be distinguished on a CT scan. Occasionally, an accessory fissure forms a physical boundary between two segments. The segments are defined based on the supply from a segmental branch of the bronchial tree. There are ten segments in the right lung and eight in the left lung. The segments form anatomical and functional regions of the lung parenchyma, and therefore pathological processes may be limited to single segments. Surgical resection can also be limited to one segment so the segmentation of these structures may be important in treatment planning.

4. CT imaging of the lungs

One of the major sources of variation when considering the performance of automatic methods to segment anatomical structures in chest CT scans is the acquisition protocol. It is therefore of vital importance to supply details about the acquisition protocol in every paper that describes segmentation methods. We discuss the most important factors here.

First of all, the section thickness and section increment need to be set when reconstructing the raw CT data. It is strongly advised to reconstruct thin-section data, with a section thickness

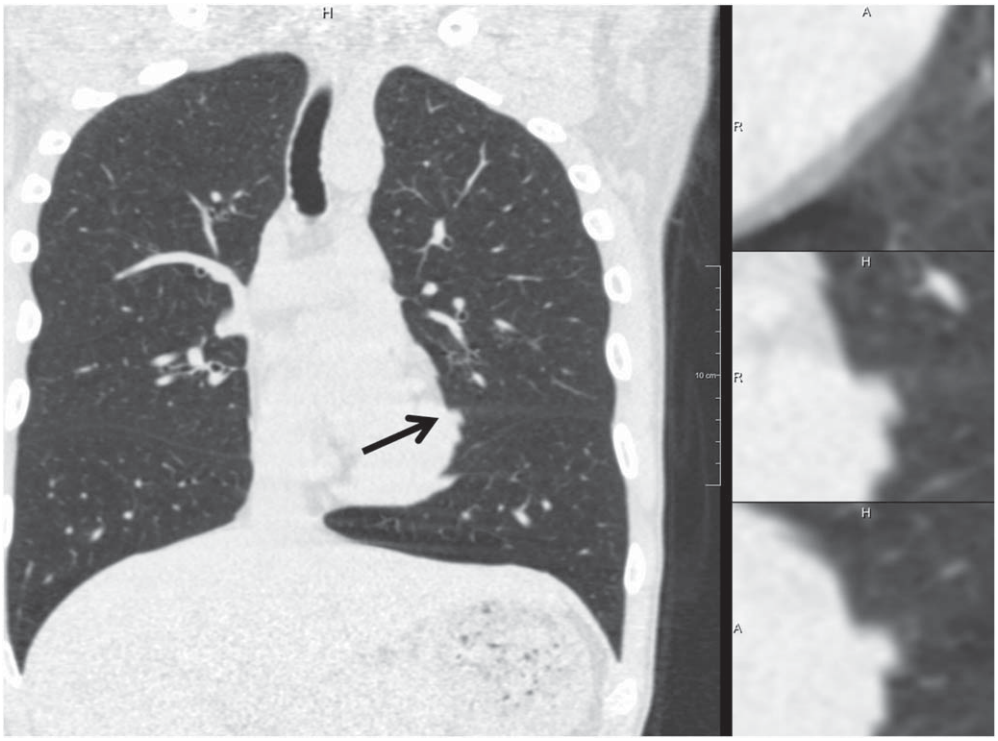

Figure 4. Illustration of cardiac motion, indicated by the black arrow. Staircase outpouchings can be seen in coronal and sagittal reformats of the data, while in the axial plane (top right), a blurry region around the heart is observed.

and spacing in the order of 1 mm. For the same acquisition protocol, reconstructing with thinner slices leads to an increase in noise, and many radiologists prefer to read axial sections that are thicker, for example 3 mm, which reduces the effect of noise. Many hospitals therefore store only such thicker sections, but this has the unfortunate side effect that valuable 3D information is lost in the process, coronal and sagittal reformations of the data look blurry and the 3D computer analysis is suboptimal or even no longer possible. Since thick sections can easily be computed from thin sections on the fly by viewing software, but not the other way around, thin-section data should be stored always (store thin, view thick). Similarly, it is important to choose the field of view and reconstruction matrix (usually 512×512, but some centers routinely reconstruct higher resolution matrices) such that the resolution in x and y directions is in the order of 0.5–0.8 mm. Reconstructing higher resolution data sets is typically not useful as the inherent resolution of the data is limited by noise due to the low radiation dose used for most clinical applications.

Most CT scanners nowadays use multi-row detectors (these detector rows are typically referred to as 'slices'). For chest imaging, excellent results can be achieved even on a four-slice scanner, but scanners with more detector rows can scan quicker. This reduces the chance that patients do not hold their breath and the scan contains breathing artifacts. For this reason, it is always advised to start the scan below the lungs and scan upward (caudal cranially) because the lower parts of the lungs move much more when the subject would suddenly start breathing and these typically already have been scanned when scanning caudal cranially. Artifacts can also be seen around the cardiac border (see figure 4), unless the scan is acquired with prospective

cardiac gating, which is typically not done for chest CT. With older single slice scanners, scanning the complete chest with thin-section collimation could usually not be done within a single breath hold and it was common, especially for indications of interstitial lung disease, to acquire a 1 mm section every 10 mm. These scans with gaps are often referred to as high-resolution CT (HRCT) although this abbreviation is now also used for thin-section volumetric scans. Needless to say, these HRCT scans with gaps are not suitable for the 3D analysis and follow-up scans are depicting slightly different sections, thus making temporal comparisons very difficult.

A very important parameter is the dose. The lower the dose, the more noisy the scan will look. The exact relation between dose and noise is complex though, and beyond the scope of this paper. The two main settings that can be varied are the tube voltage (kV) and current time product (mAs). kV determines the spectrum of the x-ray beam; mAs is directly proportional to how many x-ray photons are generated. Chest CT scans with a very low dose can still have excellent image quality and low noise levels if the patient is slim. Modern CT scanners allow the selection of kV and mAs and most modern scanners offer the modulation of the mA during scanning to adjust for patient size and local anatomy (modulates on both x/y and z). The operator selects operating parameters including control parameters for the modulation (an image quality reference parameter or a reference exposure parameter). On top of this, most vendors now offer advanced reconstruction algorithms that are model-based and iterative and operate partly in the raw domain (before reconstruction) and in the image domain (after reconstruction).

Another parameter is the so-called reconstruction kernel. ‘Sharp kernels provide higher spatial resolution, but also give more noise and the characteristic overshoot–undershoot patterns around edges. Reconstructions with ‘smooth’ and standard kernels produce images with less spatial resolution but also reduced noise and possibly more reliable density values. Vendors provide their customers with a plethora of kernels, and the choice for a particular ‘kernel’ can also mean that additional proprietary image processing is applied to the scan, completely unrelated to the reconstruction algorithm. The effect of kernel, dose setting, iterative reconstruction algorithms, and so on, can have a substantial influence on the outcome of image analysis algorithms. This is illustrated in figure 5 and for example discussed in the context of emphysema quantification by Boedeker *et al* (2004).

Thoracic CT scans can be obtained without administration of intravenous contrast agent (e.g. for lung cancer screening, diffuse lung disease, interstitial lung disease, evaluation of asthma or COPD) but for several indications, an intravenous contrast agent is administered before scanning (e.g. cancer evaluation, detection of pulmonary embolisms). As a result, the density of blood is increased and arteries, and often veins as well, are brighter. The advantages are that radiologists can now better appreciate the differences between vessels and other dense structures in the lung, they can see if there are vessels within dense lesions and obstructions in the blood flow, e.g. filling defects caused by pulmonary embolisms, can be detected.

Most papers in this review address volumetric chest CT scans obtained at full inspiration. Expiratory CT scanning is also increasingly used and 4D imaging along the breathing cycle is also gaining popularity, so far mainly for radiotherapy applications.

Since the acquisition parameters described here all have a large effect on the resulting image quality, it is recommended that all papers describing segmentation methods thoroughly describe the acquisition parameters of the data used for the development and evaluation since it allows insight into the type of data for which the evaluation of the performance of the method is valid.

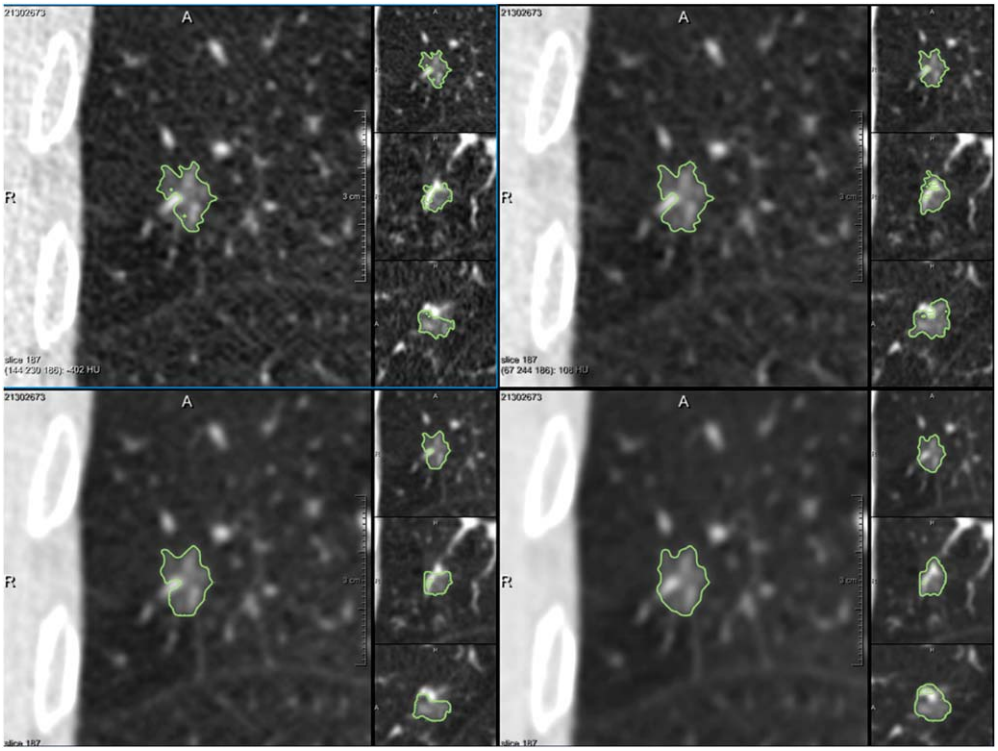

Figure 5. Illustration of the effect of reconstruction kernels and iterative reconstruction algorithms. Four different reconstructions of the same chest CT data set are displayed. The larger images are axial views. The side views show axial, coronal and sagittal reformations. The data set contains a non-solid nodule that has been segmented by an automatic segmentation method based on Kuhnigk *et al* (2006), using exactly the same settings for each reconstructed data set. Note how substantially the reconstruction settings influence the result of the computerized segmentation. The mass of the segmented lesion varies from 168 (top left) to 255 mg (top right). The scan has been acquired on a Toshiba Aquilion ONE scanner. The top row shows reconstruction with a lung kernel (FC86) which results in a slightly sharper image than the body kernel (FC09) used for the bottom row. The images on the left use standard filtered back projection. The images on the right have been reconstructed with an iterative algorithm (AIDR3D) that reduces noise while attempting to preserve tissue boundaries.

5. Lungs

5.1. Relevance

The segmentation of the lungs from chest CT scans is a prerequisite for the subsequent automated analysis since it allows for the estimation of lung volumes and detection and quantification of abnormalities within the lungs. In case of erroneous lung segmentation, findings might be missed or findings outside the lungs might be included in the analysis. Armato *et al* (2004) illustrated the importance of accurate lung segmentation for the automated detection of nodules. A standard lung segmentation algorithm was applied to a set of 60 scans followed by the automated nodule detection within the lungs. Due to erroneous lung segmentations, 17% of nodules were excluded from the lung regions and as a consequence not detected. After the lung segmentation algorithm was adapted for the specific task, the results improved to only 5% of nodules missed.

5.2. Methods

In chest CT scans of healthy subjects, lung parenchyma has a substantially lower attenuation than the surrounding tissue. As a result, the core functionality of many lung segmentation algorithms is based on a thresholding approach (e.g Armato and Sensakovic 2004, Leader *et al* 2003, Hu *et al* 2001, Sun *et al* 2006, Brown *et al* 1997, 2000). These threshold-based methods perform well in chest CT scans of patients with normal lungs but often fail in CT scans where dense pulmonary abnormalities or artifacts are present by excluding these areas from the segmentation. Other methods are specifically designed to handle such abnormalities, but are often too slow or too specialized to be used in clinical practice. Meng *et al* (2012) illustrated the performance of threshold-based lung segmentation algorithms in a large-scale robustness analysis on a set of 2768 chest CT scans of 2292 subjects with various abnormalities and scanning protocols. In all scans, an automatic threshold-based lung segmentation was performed and visually checked. In 121 scans (4.4%), the segmentation of the lungs contained errors, which in 75 scans (62%) were due to disease such as interstitial lung disease; in 39 scans (32.2%), the failures were due to artifacts from, for example, metal, and in the remaining seven cases (5.8%), the errors were caused by external factors such as corrupted dicom slices.

In this section, we will provide a short overview of the threshold-based algorithms, followed by a description of algorithms developed to overcome the problems of conventional threshold-based algorithms. Table 1 provides an overview of published journal papers with a focus on the evaluation of the proposed lung segmentation algorithms.

5.2.1. Threshold-based lung segmentation algorithms. A plethora of threshold-based lung segmentation methods has been described in the literature; therefore, we focus only on those papers published in peer-reviewed journals according to the search string provided in section 2. Some algorithms, especially older ones, are two-dimensional and process each axial section of the scan separately (e.g. Kemerink *et al* 1998, Leader *et al* 2003, Armato and Sensakovic 2004), which is a logical choice in the case of thick-slice CT data, but when isotropic data are available, 3D processing is preferable to avoid inconsistencies between slices.

Most 3D threshold-based methods for lung segmentation use similar schemes. First, the lung regions are determined, either by optimal gray-level thresholding and connected component analysis or by 3D region growing from a seed point in the trachea. For the latter, the trachea is first detected using circular region (2D) or tube detection (3D) in the top of the scan. Since the detected lung regions will contain the trachea and main bronchi, these are pruned from the result and if the lungs are connected, they are separated at the anterior and posterior junctions. Morphological operations are commonly applied to smooth the borders and include vessels in the segmentation result.

Hu *et al* (2001) were the first to publish a threshold-based lung segmentation method that operates according to scheme described above. An optimal thresholding technique was applied to find the main lung regions, followed by a connected component analysis to separate the lungs from other non-body voxels; the two largest components not connected to the border of the image were retained. The trachea and main bronchi were detected by searching for a circular region in the top of the scan as a starting point and subsequently applying closed-space dilation with a unit radius kernel (equivalent to slice-based region growing) and removed from the initial lung region. Holes in the lung regions, mainly due to vasculature, were filled by the topological analysis. In case one connected component was found for the lungs, dynamic programming was applied on a slice-by-slice basis to separate the lungs at the anterior and posterior junctions. The result was smoothed along the mediastinum using morphological operations. Ukil and Reinhardt (2005) improved upon the method proposed by Hu *et al* (2001)

Table 1. An overview of studies on the automatic lung segmentation is provided. For each study, the type of method, number of scans used for evaluation (no. of scans), evaluation method and quantitative performance are provided. RMS indicates root mean square, *D* indicates distance, HD indicates Hausdorff distance, MASD indicates mean absolute surface distance, MSBPR indicates mean signed border positioning error, *O* indicates volumetric overlap and DICE indicates the Dice coefficient.

Study	Type	No. of scans	Evaluation method	Quantitative performance
Leader *et al* (2003)	2D threshold-based	101	Comparison of lung volume to results of interactive segmentation	average difference of 95 ml for thick slice and 28 ml for thin slice data
Armato and Sensakovic (2004)	2D threshold-based	60	Effect of lung segmentation modifications on nodule detection and tumor measurements	–
Brown *et al* (1997), 2000)	3D threshold-based	104	visual inspection by a radiologist, no quantitation	–
Hu *et al* (2001)	3D threshold-based	24	RMS to manual segmentation in 229 slices from 12 scans	average *RMS* 0.54 mm
Ukil and Reinhardt (2005)	3D threshold-based	8	RMS to manual segmentation	average *RMS* 0.87 mm
Sun *et al* (2006)	3D threshold-based	20	*O* to manual delineations	average *O* 88.5%
Sluimer *et al* (2005)	Atlas-based	10	*O* to manual segmentation for proposed method, 3D threshold-based segmentation, and interactive 3D threshold-based region growing	Average *O* 82%, 39%, and 79%, respectively
Pu *et al* (2008)	Threshold-based combined with adaptive border marching	20	Volume-based over- and undersegmentation compared to semi-automatic segmentation	0.43 % and 1.63%
Prasad *et al* (2008)	Adaptive 3D thresholding	19	*O* to semi-automatic segmentation for proposed and 3D threshold-based method	88% versus 87% for TLC, 85% versus 82% for RV
Korfiatis *et al* (2008)	2D texture classification	22	*O* and RMS to manual segmentation for proposed method and threshold-based method on 140 slices	average *O* 95% versus 92%, average *RMS* 1.080 mm versus 2.345 mm, respectively
van Rikxoort *et al* (2009a)	3D threshold-based and atlas-based	150	*O* and HD to manual segmentation in 1800 slices for proposed and 3D threshold-based method	average *O* 95% versus 93%, average *HD* 23.55 versus 25.79, respectively
Wang *et al* (2009)	Threshold-based combined with texture analysis	76	*O*, mean and maximum *D* to manual delineations in 3 slices per case	averages 96.7 %, 0.84 mm, 10.84 mm, respectively
Sofka *et al* (2011)	Multi-stage learning	68	*D* to manual segmentations	average *D* 2.0 mm
Sun *et al* (2012)	3D active shape model	30	DICE, HD, MSBPR and MASD to interactive segmentation for proposed method and a threshold-based method	0.975 versus 0.949, 20.13 mm versus 33.07 mm, 0.84 mm versus 1.89 mm, 0.59 mm versus 1.25 mm

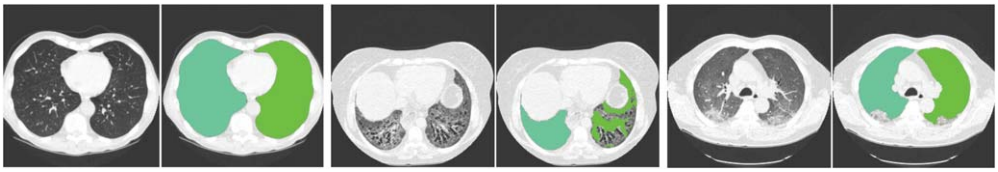

Figure 6. Illustration of the performance of conventional 3D threshold-based lung segmentation methods on scans with normal lungs and scans containing dense pathological abnormalities. The first frame provides an axial section of a scan without dense abnormalities; in the second frame, the corresponding lung segmentation is provided. The third and fifth frames show axial slices of two scans with dense abnormalities, with the corresponding lung segmentations in the fourth and sixth frames, respectively. Because of the higher densities of the abnormalities compared to the density of normal lung parenchyma, the abnormalitsies are excluded in conventional threshold-based lung segmentation methods.

by introducing a smoothing at the mediastinal area based on the airway tree to guarantee consistency among segmentations of different subjects and intra-subject over time. Sluimer *et al* (2005) and van Rikxoort *et al* (2009a) describe 3D threshold-based methods largely based on the method of Hu *et al* (2001).

Sun *et al* (2006) presented a 3D method for the segmentation of the lungs from thick-slice CT images. First, a preprocessing was applied in which the signal-to-noise ratio was improved by applying an anisotropic filter, followed by a wavelet transform-based interpolation method to construct 3D volume data. In these 3D volume data, the lungs were obtained by region growing using gray-value, homogeneity and gradient magnitude as input. Cavities inside the resulting lung region were filled using morphological closing.

Brown *et al* (1997, 2000) also applied 3D region growing and morphological smoothing operations but in addition, an anatomical model with a frame-based semantic network was used. The anatomical model modeled the chest wall, mediastinum, central tracheobronchial tree and the left and right lungs in terms of attenuation threshold, shape, contiguity, volume and relative position to allow the incorporation of anatomical variation.

5.2.2. Lung segmentation specifically designed for abnormal lungs. As illustrated in figure 6, when high density abnormalities are present in the lungs, conventional methods tend to produce errors. Sluimer *et al* (2005), Pu *et al* (2008), Prasad *et al* (2008), Korfiatis *et al* (2008), van Rikxoort *et al* (2009a), Wang *et al* (2009) and Sun *et al* (2012) developed methods to handle such abnormalities. Each method was generally developed with a specific disease in mind and therefore these methods are highly specialized and generally not tested on a large population.

Sluimer *et al* (2005) employed an atlas-based segmentation of severely pathological lungs. A probabilistic atlas was created by registering 15 chest CT scans containing lungs without abnormalities to a reference atlas and averaging the results. The segmentation of a new case was initialized by elastically registering the probabilistic atlas to the scan and transforming the lung labels. The resulting segmentation was refined by applying a voxel classification trained with data from the scan itself around the border of the lungs.

Pu *et al* (2008) developed a lung segmentation method aimed at including juxtapleural nodules in the lung segmentation since these are often not included in conventional threshold-based segmentations. The method starts with a threshold-based lung segmentation consisting of a smoothing, a thresholding at −500 HU and a slice-by-slice flooding of non-lung regions. The lung border of this initial segmentation was tracked in each axial slice and adaptive border

marching was applied to include nodules while minimizing oversegmentation into adjacent structures.

Prasad *et al* (2008) developed a method for lung segmentation in cases with diffuse lung disease to overcome the erroneous exclusion of diseased regions from the segmentation. The proposed method is a conventional threshold-based approach in which the threshold was adapted for each individual patient. To adapt the threshold, the curvature of the ribs was automatically detected and the threshold used adapted until the curvature of the lung along the rib boundary was similar to the curvature of the ribs. A clear disadvantage of this method is that while adapting the threshold optimally near the ribs, the method might lead to oversegmentation at the mediastinum.

Korfiatis *et al* (2008) used texture classification for the segmentation of lungs affected by interstitial pneumonia in 2D slices of 3D chest CT scans. The method was initialized with a *k*-means clustering based on density from which the cluster with the lowest average density was taken as the lungs. This initial segmentation does not include areas of dense abnormalities. To include possible areas that should be in the lung segmentation, an iterative approach was used in which pixels around the border of the initial segmentation were classified with a support vector machine using gray-level and wavelet coefficient statistics features.

van Rikxoort *et al* (2009a) proposed a hybrid lung segmentation approach. The rationale behind the approach was that threshold-based lung segmentation methods perform well in a large number of cases and are fast but often fail in scans where dense abnormalities are present. Specialized methods generally work better but are too time consuming to be applied to every scan in clinical practice. The method starts by applying a region-growing-based lung segmentation similar to Hu *et al* (2001). Segmentation failure was automatically detected based on the statistical deviation from a range of volume and shape measurements and to scans with failures a multi-atlas-based algorithm using non-rigid registration was applied.

Wang *et al* (2009) proposed a method for the segmentation of lungs affected by moderate to severe interstitial lung disease. They started by eliminating the airways and estimating an initial lung segmentation using thresholding techniques. This initial lung segmentation will not include regions in the lungs affected by interstitial lung disease since their density is different from normal lung parenchyma. To identify the abnormal lung regions, texture features were obtained from the co-occurrence matrix. The abnormal regions identified using the texture analysis were added to the initial lung segmentation. 2D hole filling was applied to smooth the final lung segmentation.

Sofka *et al* (2011) proposed a method that utilizes knowledge of other structures visible in the chest CT scan (ribs, carina) in a multi-stage learning-based approach which starts by identifying the carina in the trachea. The location of the carina was used in a hierarchical detection network to predict pose parameters of left and right lungs followed by the detection of a set of landmarks near the lung borders mainly on ribs and the spine. A shape model was initialized using these landmarks and was refined using a freeform refinement.

Sun *et al* (2012) developed a lung segmentation method aimed at including large tumors that are generally missed in threshold-based lung segmentation schemes. Offline, a shape model of normal lung shapes was trained using 41 scans with segmented lungs. To initialize the shape model in a new scan, automatically detected ribs were used. A robust matching approach was applied to generate a segmentation from the initial shape model. Fine details in the segmentation border not captured by the shape model were recovered using a graph-cut approach.

5.3. Challenges

Many methods for the automatic lung segmentation have been proposed and the segmentation of the lungs without abnormalities in scans of good image quality is possible with high accuracy in most cases. However, the segmentation of the lungs in cases containing pathological abnormalities remains challenging and all of the proposed methods will likely fail in a subset of cases. In 2011, a grand challenge on the segmentation of the lungs from chest CT scans was held (LOLA11, www.lola11.com) in which eight different methods participated. The grand challenge provided 55 chest CT scans from different sources containing different pathological abnormalities. The results showed that most methods performed very well on cases with healthy or emphysematous lungs but cases with severe abnormalities were incorrectly segmented by all methods. In addition, there was little variation in the performance of the different methods.

For the integration into clinical practice, the robustness of the methods is very important since radiologists need to trust the outcome of the algorithm. A large step toward the integration into clinical use might be algorithms that are robustly able to indicate potential failure, a first proposal toward this was made by van Rikxoort *et al* (2009a), and next allow effective interactive methodology to correct the segmentation in reasonable time. Several generic interactive methods are available in the literature but the interactive segmentation of the lungs from chest CT scans has received little attention in the literature so far. Kockelkorn *et al* (2010b) proposed an interactive method for the lung segmentation in which the lungs were automatically subdivided into small volumes of interest (VOIs) with homogeneous texture. After automatically segmenting the lungs in a single slice using a trained *k*-nearest neighbor classifier, the user can relabel VOIs mislabeled as lung or background. Based on the interaction of the user, a new *k*-nearest neighbor classifier is trained online to segment the lungs in the rest of the scan. The user is shown subsequent slices and can relabel VOIs until satisfied; after every slice, the classifier is retrained until the user is satisfied with the results and there is no need to relabel VOIs anymore. On a set of 12 scans for which a threshold-based lung segmentation method failed in six cases, the efficiency of the method was shown.

Three of the discussed methods used cues from other structures present in a chest CT scan, namely the ribs and vertebrae, to find the lung borders more reliably (Prasad *et al* 2008, Sofka *et al* 2011, Sun *et al* 2012). Since the position of anatomical structures in the thorax is related, this seems a very promising approach and availability of more and more automated segmentation of several anatomical structures allows this type of integration. In addition, the segmentation of other anatomical structures might also help indicate to the lung segmentation method if the resulting segmentation is possibly erroneous, for example by checking the height of the lungs compared to the ribs.

6. Vessels

6.1. Relevance

The segmentation of the pulmonary vessel trees allows the detection of vascular abnormalities as well as the exclusion of normal vasculature from the analysis of dense abnormalities in the lungs (e.g. Korfiatis *et al* 2011). Automatic segmentation of the pulmonary vessels is often used in CAD systems, for example, to reduce the number of false positives in a nodule detection system (Agam *et al* 2005). Since the different lobes in the lungs are provided by different parts of the vessel tree, the vessels can also be used to guide the segmentation of the lobes and segments or guide registration methods.

The separation of the segmented vessel tree into arteries and veins can, for example, be useful for algorithms being used to detect pulmonary embolisms (Zhou *et al* 2007) and determine pulmonary hypertension. The separation of the vascular trees in the lungs into arterial and venous trees is challenging since the differentiation between bifurcations and crossings is far from trivial, especially in non-contrast enhanced scans. In a survey from 2006 on the lung image analysis (Sluimer *et al* 2006), the separation of arterial and venous trees in the lungs was mentioned as 'one of the main future challenges'. Two publications about artery–vein separation in chest CT scans appeared since this survey (Bülow *et al* 2005, Saha *et al* 2010).

6.2. Methods

We focus solely on methods segmenting the complete pulmonary vessel trees. For an overview of general vessel enhancement and segmentation methods, we refer to Lesage *et al* (2009). The segmentation of the vessel trees in the lungs is commonly performed using one of the following three schemes: thresholding, vesselness filters, or tree growing or tracking. In this section, each of the three approaches will shortly be described and studies applying the described techniques discussed, followed by a description of the methods available for the separation of arteries and veins.

The evaluation of vessel segmentation in the lungs is difficult since there are a lot of vessels in the lungs, rendering it impossible to have all vessels manually delineated in a large set of scans. In studies where the vessel segmentation is not the main goal, vessels are often segmented by simple thresholding and the performance of the vessels segmentation is in these studies not assessed. For the evaluation of other methods, several strategies have been employed; some methods were evaluated by comparing to complete manual segmentations in few scans (e.g. Zhou *et al* 2007), other methods were evaluated in terms of their benefit for CAD systems (e.g. Agam *et al* 2005, Korfiatis *et al* 2011), and most methods compared to manually indicated points inside the vessels for a larger set of scans (e.g. Ochs *et al* 2007, Shikata *et al* 2009, van Dongen and van Ginneken 2010, Lo *et al* 2010, Korfiatis *et al* 2011, Zhou *et al* 2012). An overview of the evaluation methodology and results of the different vessel segmentation methods is provided in table 2.

6.2.1. Thresholding. In cases in which no dense abnormalities are present, the vessels can be segmented with a simple density thresholding approach, which is often applied in papers where the segmentation of the vessels is auxiliary to the main task such as lobar segmentation (e.g. Lassen *et al* 2013).

6.2.2. Vesselness. The most common approach to vessel segmentation is the use of filters based on eigenvalues of the Hessian matrix or the structure tensor. This type of structure enhancement was initiated by Koller *et al* (1995) who described a Hessian-based analysis for the detection of curvilinear structures and Haussecker and Jähne (1996) who introduced the use of the structure tensor for the local structure analysis. Frangi *et al* (1998) were the first to explicitly describe the construction of a vesselness measure using a combination of all eigenvalues of the Hessian matrix. The eigenvalue analysis of the Hessian matrix provides the principal directions in which the local second-order structure can be decomposed. Hessian-based vesselness filters employ the grayscale curvature characteristics of bright tubes against a dark background, where one expects one vanishing curvature parallel to the tube and two strong curvatures perpendicular to the tube. Using these curvature expectations, a filter can be constructed to enhance vessels while suppressing other structures such as blobs (three strong

Table 2. An overview of studies toward automatic pulmonary vessel segmentation is provided. For each study, the type of method, number of scans used for evaluation (no. of scans), the use of contrast material, evaluation method and quantitative performance are provided. TP(F) indicates true positive (fraction), FP(F) indicates false positive (fraction) and FN indicates false negative.

Study	Method	No. of scans	Contrast	Evaluation method	**Quantitative performance**
Agam *et al* (2005)	Correlation-based vesselness + tree reconstruction	38	no	Comparison to manual tagging in five cases to detect FN, influence on FP in nodule CAD	average 1% FN, 38% reduction in FP CAD responses
Zhou *et al* (2007)	Vesselness	2	yes	Accuracy compared to manual vessel tracking	97% and 94% for the two cases
van Dongen and van Ginneken (2010)	Vesselness	10	no	Sensitivity and specificity compared to manually labeled points as TP and FP	sensitivity 0.71 at specificity 0.94
Ochs *et al* (2007)	AdaBoost classification	29	mixed	Area under the ROC curve compared to 19,000 manually labeled points	area under the curve 0.953 ± 0.016
Korfiatis *et al* (2011)	Vesselness and supervised classification	7	–	TPF and FPF compared to manual segmentation in 30 slices per case for proposed method and (Zhou *et al* 2007).	0.935 & 0.074 versus 0.968 & 0.400
Xiao *et al* (2011)	Generalized vesselness	2	no	Manual labeling in VOIs around the fissures, area under precision/recall curves for both scans, compared to traditional vesselness	0.822 and 0.813 versus 0.693 and 0.612
Bülow *et al* (2005)	Wavefront propagation	–	–	Visual inspection, not quantitatively evaluated for pulmonary vessels	–
Shikata *et al* (2009)	Vesselness and tracking	44	no	$>$ 1000 manually placed TP and FP points per scan	average 99% TP, 1% FP
Lo *et al* (2010)	Locally optimal paths	10	no	Comparison of tree length extracted to thresholding vesselness, no TP,FP analysis	average 55.61m versus 52.17m extracted
Zhou *et al* (2012)	CPR optimal paths	8	yes	Comparison to manual vessel segmentation in volumes of interest in terms of volume error and inter-class correlation	$9.9 \pm 7.9\%$ and 0.988

curvatures expected) and plates (only one strong curvature expected). A segmentation of the vessels can be obtained afterward by thresholding the filter output, commonly followed by morphological operations and/or connected component analysis. Variations on this approach have been proposed by several researchers to detect the vessels in the lungs, e.g. Agam *et al* (2005), Zhou *et al* (2007), van Dongen and van Ginneken (2010).

Some researchers proposed different approaches to vesselness filtering. Ochs *et al* (2007) did not explicitly model the vesselness but used the eigenvalues of the Hessian matrix in a pattern recognition approach to detect the vessels. Korfiatis *et al* (2011) started with a vesselness filter followed by a supervised classification using texture features obtained from the co-occurrence matrix to correct possible oversegmentations due to abnormalities. Xiao *et al* (2011) presented a strain energy vesselness filter, designed to overcome the strict tubular structure enhancement of common Hessian-based filters to also enhance bifurcations. The method provides a generalized vesselness filter describing brightness, structure strength, intensity continuity and vascular shape discrimination in a multiscale framework.

6.2.3. Growing and tracking. Since the vessels in the lungs form two trees, the arterial and venous trees, several researchers applied tree reconstruction algorithms such as region growing or wavefront propagation. The tree reconstruction can be performed on the original CT data but is also often initialized using a vesselness filter. Bülow *et al* (2005) proposed a general tree extraction framework ((Bülow *et al* 2004), inspired on (Schlathölter *et al* 2002)) that was applied to the segmentation of pulmonary vessel trees. The method starts from a set of seed points from which a fast marching front propagation was started, accepting voxels above a certain density threshold. The front was regularly checked for connectivity, when the front splits, a bifurcation in the tree was detected and the expanding of the current tree segment finished. The tree segments were evaluated during segment growth and rejected if their radius exceeded certain maxima, indicating a leakage.

Shikata *et al* (2009) started their segmentation process with the output of a vesselness filter. Since thresholding the output of the vesselness filter may lead to disconnected vessels, especially around bifurcations, the output of the vesselness filter was not directly thresholded but used to set seed points in the middle of vessel segments for a vessel traversing approach. From the seed points, trajectories were made to the nearest junction to connect possibly disconnected vessel segments.

Lo *et al* (2010) proposed a method to segment the pulmonary vessel trees using locally optimal paths. A vesselness filter was applied as the basis of the algorithm. Local maxima in vesselness were taken as seed points and spheres around the seed points were defined in which the Dijkstra algorithm was applied, using a cost function based on the vesselness, to obtain vessel candidate paths. From the obtained vessel candidate paths, the optimal paths were selected based on criteria related to vesselness, shape, orientation and distance from other paths.

Zhou *et al* (2012) proposed a method to segment the pulmonary vessels using locally optimal paths in curved planar reformations (CPRs). The method was initialized with a Hessian-based vesselness filter (Zhou *et al* 2007). The vessels detected in the vesselness filter were straightened in the CPR volume and segmented using adaptive thresholding. Optimal paths were traced based on Dijkstra's algorithm.

6.2.4. Artery–vein separation. Bülow *et al* (2005) proposed a method to separate the arteries and veins in the lungs given segmentations of the vessels and bronchi. The method utilized the fact that arteries and bronchi accompany each other in the lungs by determining if a vessel

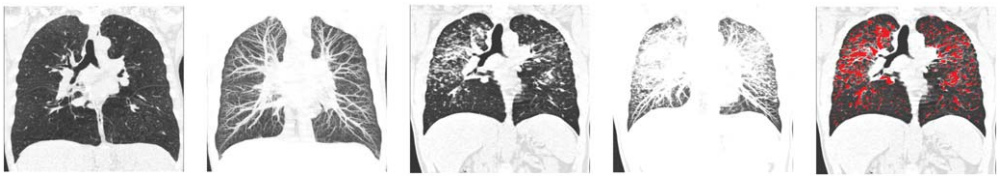

(a) (b) (c) (d) (e)

Figure 7. Examples of thin slices ((a) and (c)) and their maximum intensity projections over 4.5 cm ((b) and (d)) and a vessel segmentation result (e). (a) and (b) were taken from a scan that does not contain dense abnormalities, (c)–(e) were taken from a scan with dense abnormalities due to interstitial lung disease. It can be seen that when no dense abnormalities are present, the maximum intensity projection nicely depicts the vessels, indicating that the vessels can be extracted by a simple threshold-based technique. However, when abnormalities are present, the vessels cannot be distinguished from the lung parenchyma in this way. (e) illustrates the result of a thresholded vesselness filter; it can be observed that the resulting vessel segmentation includes both vessels and parenchymal abnormalities.

segment is close to a bronchus running in parallel orientation. The method was only visually evaluated.

Saha *et al* (2010) proposed a semi-automatic method for the segmentation of arteries and veins employing multiscale topomorphologic opening operations at locations where two vessels were fused. The method was evaluated using a phantom and two chest CT scans in which human observers manually indicated over 8000 points inside a vessel segmentation as being artery or vein to serve as a reference standard. The results indicated that a 95% accuracy was achieved for the two scans when between 25 and 40 seeds were manually placed for both arteries and veins.

6.3. Challenges

The automated segmentation of the vessels in the lungs has received relatively little attention in peer-reviewed journals, mainly due to the difficulty to properly validate vessel segmentation algorithms and the fact that in cases without dense pulmonary abnormalities, the vessels can be identified rather well by simple thresholding. However, in cases with abnormalities, this thresholding would fail completely. This is illustrated in figure 7, where the result of a vesselness filter on a case with dense abnormalities is also depicted. Korfiatis *et al* (2011) were the first to specifically attempt to develop a vessel segmentation method able to handle interstitial lung disease by including a voxel classification to exclude oversegmentation, but evaluation was limited to seven cases. Robust segmentation of the pulmonary vessels in scans containing gross pathologic abnormalities remains an open research area. In a recent grand challenge for pulmonary vessel segmentation (VESSEL12, http://vessel12.grand-challenge.org), a set of scans obtained from subjects varying from healthy subjects to subjects with pathological abnormalities such as emphysema, nodules and pulmonary embolisms were provided and 19 different vessel segmentation algorithms were compared. The reference standard was obtained by manually labeled points inside vessels and abnormalities. The results showed that even the best methods performed poorly in areas where dense abnormalities were present and included these in the vessel segmentation.

The separation of arteries and veins is important for several clinical questions, e.g. Wittenberg *et al* (2012) showed that many false positives of a CAD system for the detection of pulmonary embolisms occurred in the veins, while emboli can only occur in the arteries.

These kinds of errors not only increase the false-positive rate but also lead to less confidence of CAD by radiologists since these are obvious false positives they would never consider themselves. Only two methods for the artery–vein separation in the lungs are available (Bülow *et al* 2005, Saha *et al* 2010) but they were not properly evaluated and/or require user interaction. Therefore, the separation of pulmonary arteries and veins remains a challenge. The method proposed by Bülow *et al* (2005) included anatomical knowledge and the method proposed by Saha *et al* (2010) provides an elegant theoretical framework to separate vessels that appear attached at the resolution of a chest CT scan. A framework combining both approaches might provide a next step toward automatic artery–vein segmentation.

7. Airways

7.1. Relevance

Automated segmentation of the bronchial lumen and wall from thoracic CT scans is a prerequisite for the analysis of airway disease: the airway lumen and wall dimensions are often used to quantify the severity of airway disease in e.g. COPD, asthma and cystic fibrosis. The separation of the airway wall and lumen is a very challenging task since the walls are really thin, below the resolution of the scan at many locations, and often obscured by partial volume effects, noise, or pathological processes. In addition, the location of the airway tree can aid other segmentation tasks such as the subdivision of the lungs into lobes and segments. In the past year, both an extensive review on automated airway analysis (Pu *et al* 2012) and an overview paper of a grand challenge toward airway segmentation (EXACT09, http://image.diku.dk/exact) (Lo *et al* 2012) have been published. We therefore refer to these papers for an extensive overview of published works and methodology. In this section, we will discuss common approaches and challenges for the segmentation of the airway wall and airway lumen.

7.2. Methods

7.2.1. Airway lumen segmentation. Since on a chest CT scan, the airway lumen presents as a dark tube surrounded by a bright airway wall, a common approach to segment the airway lumen is to use variants of gray-value-based region growing, e.g. Mori *et al* (1996), Sonka *et al* (1996), Mori *et al* (2000), Swift *et al* (2002), Aykac *et al* (2003), Kiraly *et al* (2004), Bülow *et al* (2004), Fetita *et al* (2004), Tschirren *et al* (2005), Palágyi *et al* (2006), Graham *et al* (2008), van Ginneken *et al* (2008). These approaches perform very well in areas where the airway wall is clearly distinguishable on a chest CT scan. However, the airway wall might locally be obscured due to noise or partial volume effects or not intact due to pathological processes such as emphysema. In these areas, airway lumen segmentation techniques only relying on the intensity-based segmentation often ‘leak’ into the lung parenchyma surrounding the airways, leading to false airway branches. Several approaches have been proposed to prevent region-growing-based methods from leaking into the lung parenchyma. Mori *et al* (1996) proposed ‘explosion-controlled region growing’, which is an iterative region-growing method in which the threshold value is increased until the airway volume ‘explodes’. The tree grown with the threshold before explosion is retained. Schlathölter *et al* (2002) extended this idea by stopping the segmentation locally where leakage occurs, while allowing the segmentation to continue in other regions. A second problem with conventional region growing is that when the airway lumen locally has a higher density on the CT scan, for example due to the presence of noise

in the scan or mucus in the airways, conventional intensity-based region-growing approaches will stop and not detect distal airway branches.

The problems with intensity-based region-growing-based methodology have sparked several researchers to investigate different techniques to segment the airway lumen. Bronchi enhancement filters can be designed using the analysis of the Hessian matrix as described for vessel segmentation. Ochs *et al* (2007) used an eigenanalysis of the Hessian matrix as features in a pattern recognition approach, like for vessel segmentation. Tschirren *et al* (2005) used a fuzzy connectivity approach in which adaptive cylindrical regions of interest followed the airway branches during the segmentation by updating their orientation, size and position. Within the current region of interest, the airway segmentation was performed, allowing leakages to be detected early. Sonka *et al* (1996) and Lo *et al* (2010) employed the segmentation from vessels running parallel to the bronchi to improve segmentation results. Sonka *et al* (1996) incorporated the proximity of vessels into a region-growing approach. Lo *et al* (2010) used a pattern recognition approach using spatial derivatives through second order and Hessian eigenvalues and ratios between them as features to construct an airway probability for each voxel. Next, an vessel orientation similarity measure was computed for each voxel and combined with the airway probability in a region-growing approach. The method proposed by Lo *et al* (2010) tackles leakage with the airway probability and early termination of the airway tree segmentation with the vessel orientation measure. Pu *et al* (2011) used a differential geometry approach which modeled all anatomical structures using matching cubes and subsequently used principal curvatures and directions to differentiate between bronchi and other structures in geometric space to overcome the problems of intensity-based region-growing approaches.

7.2.2. Airway wall segmentation. Methods to segment the airway wall can roughly be categorized into 2D and 3D methodologies. 2D airway wall segmentation methods are either applied directly on axial slices but preferably image planes are reformatted perpendicular to the centerline of the airway lumen. Full width at half-maximum (FWHM) is a commonly used 2D approach for airway wall thickness measurements which assumes that the walls of the lumen and wall are located halfway between the maximum within the airway wall and the minimum in the lumen or lung parenchyma. FWHM is applied in 2D sections, by shooting rays from the center of the lumen and studying the intensity profiles (Reinhardt *et al* 1997, Nakamura *et al* 2000). The FWHM method is highly dependent on, among other things, reconstruction kernel and airway size. To overcome this problem, Reinhardt *et al* (1997) proposed a model for the intensity profiles of rays from the airway lumen center based on the scanning process that was fitted to the CT data. The method performed better than FWHM but required calibration for each set of acquisition parameters. Several other 2D airway wall segmentation methods have been proposed since then, for example, based on phase congruency (Estépar *et al* 2006), intensity integration (Weinheimer *et al* 2008, Schmidt *et al* 2010), or model fitting (Odry *et al* 2006). Although when resampling perpendicular to the airway direction, the segmentation of the airway walls can be performed throughout a segmented airway tree, 2D methods inherently suffer from inconsistencies between slices and are incapable of producing correct results around branching points.

To overcome this, several 3D airway wall segmentation methods have been proposed. Liu *et al* (2009) started from an existing airway lumen segmentation mesh and subsequently used an optimal graph search algorithm to simultaneously segment the lumen and airway wall boundaries. Petersen *et al* (2011) proposed a new graph construction technique for the multi-surface segmentation based on non-intersecting flow lines to be able to handle large curvatures

as observed in the airway tree. Gu *et al* (2013) proposed a 3D active surface evolution that minimizes an energy function containing external and internal energy functions to be balanced.

7.3. Challenges

A large amount of airway tree segmentation methods have been proposed in the literature over the last 16 years. The evaluation of airway tree segmentation methods is challenging since manually segmenting complete airway trees is not feasible. The EXACT09 grand challenge therefore used a clever method in which segmented airway branches were visually scored by human observers as being airway or non-airway for all methods and the results combined into a reference standard. Evaluating the results of 15 submitted methods on 20 chest CT scans with varying abnormalities and obtained with varying scanning protocols showed that on average none of the methods was able to detect more than 74% of all airways. Combining the results of all methods, this increased to 78.8% from which the organizers concluded that there is complementary information in the different methods but also that there is room for improvement. In general, the evaluation of airway segmentation methods on scans with gross pathological abnormalities or obtained at full expiration and/or with (ultra-)low dose is rare. The segmentation of the airway wall received less attention so far, but is even more challenging to evaluate due to the small dimensions of the airway wall. Several authors have used phantom measurements to evaluate their algorithm, next to comparison to FWHM at selected slices and correlations with pulmonary function testing.

8. Fissures

8.1. Relevance

There are two types of pulmonary fissures: lobar fissures and accessory fissures. The lobar fissures delineate the lobes in the lungs and are important for the localization of disease and can stem disease spread between the lobes. Incomplete fissures can cause collateral flow between lobes and render certain bronchoscopic intervention of chronic lung diseases ineffective. Accessory fissures are a cleft of varying depth lined by visceral pleura (Ariyürek *et al* 2001). Accessory fissures most often occur between pulmonary segments but may also enter subsegmental or interbronchial planes. Most of the automatic fissure detection method aim at only detecting the lobar fissures. The segmentation of the pulmonary fissures from chest CT scans has only become feasible with the advent of multi-detector CT scanners, allowing thin-section CT imaging of the entire lungs in a single breath hold. Since the fissures are thin surfaces in the lungs, on thick-section CT scans, the fissures are only visible as vague bands of increased density due to partial volume effect.

8.2. Methods

The most common approach to pulmonary fissure detection is filters based on eigenvalues of the Hessian matrix or the structure tensor as described for vessel segmentation. Several authors proposed modifications of the vesselness measure proposed by Frangi *et al* (1998) to enhance plates such as the fissures (Sato *et al* 2000, Li *et al* 2003). For the detection of fissures from chest CT scans, the use of these filters was first proposed by Wiemker *et al* (2005), who presented two filters for the enhancement of all pulmonary fissures, one based on the analysis of the eigenvalues of the structure tensor and another based on the eigenvalues of the Hessian matrix. No quantitative analysis was performed but both filters visually performed similarly according to the authors. Lassen *et al* (2013) presented a slightly different Hessian

eigenvalue-based fissure enhancement filter in which not only the plateness of the fissure was taken into account but also the strength of the image structure for better differentiation between vasculature and fissures. The fissure enhancement filter was not separately evaluated since it was part of a lobar segmentation method. Ochs *et al* (2007) proposed a pattern recognition approach to detect all pulmonary fissures. An ensemble classifier was trained on manually provided points in fissures, vessels and airways. Eigenvalues of the Hessian matrix and their combinations were used as features. The method was evaluated on a set of 29 chest CT scans from different sources and shown to reach an area under the ROC curve of 0.95 on average. van Rikxoort *et al* (2008) also proposed a pattern recognition approach to enhance the pulmonary fissures. The eigenvalues of the Hessian matrix were used as features in combination with first- and second-order image derivatives. A two-step classification was performed trained on manually delineated fissures. The method was quantitatively evaluated on a set of 22 scans with manual segmentations of the fissures and shown to perform well, with an area under the ROC curve of 0.98 compared to 0.90 for the method by Wiemker *et al* (2005) which was implemented for comparison.

Methods aimed at only locating the lobar fissures, usually as a prerequisite for a subsequent lobar segmentation, commonly start by defining an approximate location of the lobar borders based on prior anatomical knowledge to limit the search area for fissure detection. Zhang *et al* (2006) employed an anatomical lung atlas constructed using CT data of 16 subjects to initialize fissure segmentation. The fissures in the initial area were enhanced in each axial section using a 2D ridgeness measure. This information was combined in a fuzzy logic system to extract the final fissure positions for the major fissures in left and right lungs. An evaluation on 22 chest CT scans was performed by comparing the output of the method to manual tracings of the fissures in terms of root mean square (RMS) error. The RMS error for fissure segmentation was computed employing only the distance between each point on a manually segmented reference fissure and the automatically segmented fissure. The RMS error for fissure segmentation is commonly performed in this manner since the reference segmentations often only include the lobar fissures, where methods might also segment accessory fissures. The RMS error between the method and manual tracings was 1.96 mm on average. Wang *et al* (2006) presented a method to segment the lobar fissures that started with a manual initialization in one axial section of a chest CT scan located in the lower half of the lung. Starting from this axial section, key axial sections were identified throughout the lung in which the fissures were segmented. The manually traced fissure in the first section was transformed to the next closest key axial section to initialize a fissure search region and shape prior. Within the fissure region, a ridgeness map was computed which, combined with the shape prior, was used in a curve growing method to delineate the fissure in the section. This process was repeated until the fissure in all key sections was segmented, at which point a 3D linear interpolation was applied to segment the fissure in all sections of the scan. The method was evaluated on ten chest CT scans on which fissures were manually traced. The average distance between the automatically delineated fissure and the manual tracing was 1.01 mm; in 2.4% of sections, manual correction was applied. Ukil and Reinhardt (2009) combined a distance transform to segmented vessels and the original chest CT scan as a cost image for a watershed transform guided by airway and vascular markers. Based on the watershed segmentation, an initial search area for the pulmonary fissures was determined. In the search area, a ridgeness measure based on the structure tensor analysis was applied on transversal slices followed by a 3D graph search to locate the optimal surface within the search area to be the pulmonary fissure. The method was evaluated by comparing to manual tracings of the fissures in scans of 12 normal subjects imaged at inspiration and expiration and 17 patients with emphysema imaged at full inspiration. The RMS errors for the left major, right major and right minor fissure were 1.81, 1.57 1.43 mm for the inspiration data

of the healthy subjects and 1.71, 1.88 and 2.31 mm for the data of the emphysematous patients, respectively. Pu *et al* (2009a) presented a geometrical approach to fissure detection in chest CT scans which does not incorporate anatomical knowledge other than a segmentation of the lungs. As a first step, all voxels in the lungs were thresholded between −800 and −400 HU. To enhance the pulmonary fissures while depressing non-fissure structures, Laplacian smoothing was applied and the fissure was represented by small planar patches. Planar patches were classified into fissural or non-fissural and later unified into fissure surfaces. The method was compared to manual tracings of fissures on 100 slices from ten chest CT scans and shown to have an average RMS of 2.0 mm for two observers.

8.3. Challenges

Several methods for the automatic segmentation of the pulmonary fissures have been presented that all show almost sub-voxel precision as compared to manual fissure tracing in a small set of evaluation cases. Although slightly different approaches have been used for different studies, all approaches start from a plate or ridgeness filter potentially combined with anatomical knowledge and/or post-processing steps to remove false responses. The main challenge for fissure segmentation in the coming years will be to prove robustness of the methods, or a combination of the methods, on large databases and to evaluate and possibly improve the performance on cases with pathological abnormalities that interfere with the course of the fissure or alter the appearance of the fissure. The main application for fissure segmentation is to aid the segmentation of the pulmonary lobes, which is discussed in the next section.

9. Lobes

9.1. Relevance

The five pulmonary lobes are physically separated by the pulmonary fissures. In case a pulmonary fissure completely delineates the border between two lobes, the segmentation of the different lobes is trivial if an accurate segmentation of the pulmonary fissures is available. However, pulmonary fissures are not only challenging to segment but the pulmonary fissures have also been shown in several studies to frequently be incomplete. In a study on 100 lung specimens, Raasch *et al* (1982) found incomplete fissures in 46% of the left lung specimens, 70% of the right major fissures were incomplete and 88% of the right minor fissures were incomplete. Aziz *et al* (2004) and Gülsün *et al* (2006) examined the pulmonary fissures on 622 and 144 chest CT scans and both observed substantial numbers of incomplete fissures. Figure 8 illustrates the lobar segmentation in a scan with complete and a scan with incomplete fissures.

The segmentation of the pulmonary lobes allows the localization and quantification of the heterogeneity of pulmonary diseases. The amount of disease activity can vary substantially between the lobes, and some diseases generally affect only the upper or lower lobes. The heterogeneity of the disease over the different lobes allows the quantification of the spread of the disease and might affect treatment planning. For example, lung volume reduction surgery (LVRS) has been shown to be significantly more effective in cases of heterogeneously distributed emphysema with most emphysema in the upper lobes than in homogeneously distributed emphysema. There are currently bronchoscopic lung volume reduction (BLVR) alternatives to LVRS, where the preference for several techniques depends on the heterogeneity of the emphysema over the different lobes. A segmentation of the lobes and fissures allows

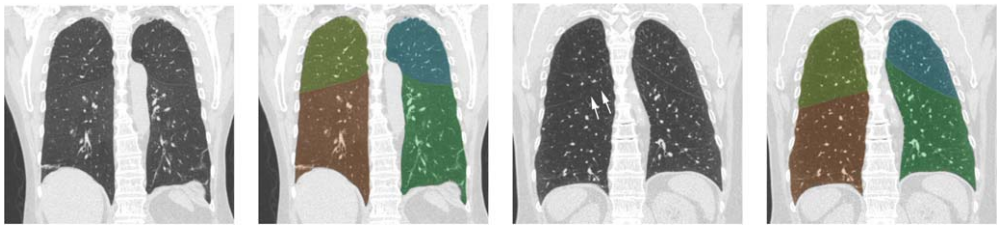

(a) (b) (c) (d)

Figure 8. A coronal slice of a scan with complete major fissures and corresponding lobe segmentation ((a) and (b)), and a coronal slice of a scan with an incomplete right major fissure and corresponding lobe segmentation ((c) and (d)). The incomplete part of the fissure is indicated with arrows in (c).

the identification of patients with incomplete fissures, which is of importance since fissures stem collateral flow and disease spread.

9.2. Methods

The lobe segmentation is a challenging segmentation task, mainly due to incomplete or difficult to distinguish fissures and anatomical variation, either naturally or due to disease altering the shape of the lobes. Several methods have been proposed to date. All methods start by segmenting the lungs and detecting the pulmonary fissures. The main conceptual difference between the methods is how areas with incomplete fissures are handled for which two main strategies can be distinguished: some methods explicitly use cues from other structures to determine the most likely position of the lobar border, while others purposely do not include such information. The first strategy is based on the rationale that the different lobes are separately supplied by different subtrees of the bronchial and vascular trees and these therefore provide useful information to locate the borders between the lobes. The rationale of not using auxiliary information from other anatomical structures is to minimize dependence on the success of automatic segmentation of these structures. An overview of proposed lobe segmentation methods and evaluation is provided in table 3.

9.2.1. Methods not incorporating auxiliary segmentations. After the automatic segmentation of the lungs and fissures, for which each paper described their own technology but generally speaking any methodology described in the sections above could be used, different authors propose different schemes to come to a final lobar segmentation. Zhang *et al* (2006) and van Rikxoort *et al* (2009b) presented methods that only used information of the lungs and fissures. Zhang *et al* (2006) initialized the location of the lobar border using 2D ridgeness detection and registering a pulmonary atlas based on lung and fissure locations. The fissure segmentation was refined using fuzzy logic. In case the (detected) fissures did not cover the complete boundary of a lobe, the method could only be run with a manual interaction. As a result, the proposed method can only be applied automatically in cases with complete pulmonary fissures. van Rikxoort *et al* (2009b) presented a voxel classification approach using distance and direction to detected fissures and location inside the lungs as features. The method handled incomplete fissures based on provided training examples, but the results in cases with severely incomplete fissures were often not satisfactory (van Rikxoort *et al* 2010).

Pu *et al* (2009b) and Ross *et al* (2010) also described methods that did not take additional information into account but the methods were specifically designed to be able to handle

Table 3. An overview of studies toward the automatic pulmonary lobe segmentation is provided. For each study, the type of method, number of scans used for evaluation (no. of scans), evaluation method and quantitative performance are provided. RMS indicates root mean square, *D* indicates distance and DICE indicates the Dice coefficient.

Study	Method	No. of scans	Evaluation method	Quantitative performance
Zhang *et al* (2006)	Atlas-based + ridgeness in 2D slices	22	Comparison to manually traced fissures in terms of RMS and DICE for the lobes	averages 1.96 mm and 0.988
van Rikxoort *et al* (2009b)	Voxel classification based on position in lobes	100	Comparison to 697 manually labeled points	97% and 90% of points correctly assigned in left and right lungs, respectively
Pu *et al* (2009a)	Fissure detection + radial basis functions in cases with incomplete fissures	65	Visual score by two observers	good or excellent in 50.8% of cases
Ross *et al* (2010)	Fissure detection + thin-plate spline	6	Comparison to manual segmentation in cases with incomplete fissures in terms of average *D*	1.80 mm, 2.23 mm, 1.90 mm
Shamonin *et al* (2012)	Fissure detection + B-spline	22	Comparison to interactive segmentation in terms of DICE at lobes (LUL,LLL,RUL,RLL,RML) and left major, right major, and right minor fissures	medians 0.99, 0.98, 0.98, 0.97 and 0.87 for the lobes and 0.65, 0.54 and 0.44 for the fissures, respectively
Gu *et al* (2012)	Fissure detection + B-spline	30	Comparison to manual segmentation in terms of RMS, mean *D*, and max *D* for left major, right major, and right minor fissures	average *RMS* 1.46 mm, 1.54 mm, 1.73 mm, respectively
Schmidt-Richberg *et al* (2012)	Fissure detection + level set	9	Comparison to manual segmentation in terms of DICE at lobes and left major, right major, and right minor fissures	averages 0.94, 0.83, 0.76, and 0.48, respectively
Nimura *et al* (2012)	Fissure detection + graph-cut	6	Comparison to manual segmentation in terms of Jaccard index	average 79.1%

Table 3. (Continued.)

Study	Method	No. of scans	Evaluation method	Quantitative performance
Agarwal *et al* (2012)	Multi-atlas	23	Comparison to interactive segmentation in terms of DICE at fissures	median 0.60
Kuhnigk *et al* (2005)	Vessels + intensity + watershed	–	No quantitative evaluation was performed	–
Ukil and Reinhardt (2009)	Fissures + airways + spline interpolation	29	Comparison to manual left major, right major and right minor fissure tracing in terms of RMS, mean *D*, and max *D* for 29 CT scans, 12 from healthy subjects and 17 from COPD patients, qualitative scoring of 10 cases with incomplete fissures	average *RMS* 2.31 mm, 1.57 mm, and 1.63 mm for healthy subjects, 1.86 mm, 2.04 mm, 1.50 mm for COPD patients, respectively. 4 out of 10 cases no errors
van Rikxoort *et al* (2010)	Fissures + airways + multi-atlas	120	Comparison to manual left major, right major, and right minor fissure tracing in terms of RMS, mean *D*, and max *D* for 20 CT scans, qualitative scoring of 100 cases with incomplete fissures	average RMS 1.28 mm, 1.88 mm, 1.98 mm, respectively. 85% scored as good or excellent for all lobar borders
Lassen *et al* (2013)	Fissures + airways + vessels + watershed	75	Comparison to manual left major, right major, and right minor fissure tracing in terms of mean *D*, and max *D* for 20 CT scans and application to LOLA11 grand challenge	averages 0.69 mm, 0.67 mm, 1.21 mm, respectively.

incomplete fissures. Pu *et al* (2009b) identified the individual pulmonary fissures and in case the fissures did not extend from lung border to lung border, implicit radial basis functions were used to extend the fissures. The method was qualitatively evaluated on 65 scans and rated as good or excellent in 50.8% of the cases by two observers, but the performance in cases with incomplete fissures was not specified. Ross *et al* (2010) started by identifying pulmonary fissure candidates using a particle filtering approach followed by maximum *a posteriori* estimation to eliminate false responses. A thin plate spline was fitted through the determined fissure candidate points to segment the lobar boundary and extend incomplete fissures. The method was specifically evaluated on six cases with incomplete fissures and performed comparable to the inter-observer variability between two pulmonologists. Similar methods to segment the lobes with complete and incomplete fissures have recently been proposed by Shamonin *et al* (2012), who employed iterative B-spline fitting that interpolates at areas where no fissure was detected, Gu *et al* (2012) who applied a quadratic B-spline weighting strategy to ensure that the segmentation is smooth, Schmidt-Richberg *et al* (2012) who applied a level set segmentation guaranteeing a closed object using a vesselness filter as a cost function and Nimura *et al* (2012) who applied a graph-cut segmentation using a sheetness filter in the cost function after registering a probabilistic atlas. Agarwal *et al* (2012) proposed a multi-atlas-based segmentation of the lobes with label fusion based on local weights (coined local multilabel SIMPLE).

9.2.2. Methods incorporating auxiliary segmentations. Kuhnigk *et al* (2005), Ukil and Reinhardt (2009), van Rikxoort *et al* (2010) and Lassen *et al* (2013) all described methods that do take information of anatomical structures into account. The first paper on the automatic lobar segmentation was presented by Kuhnigk *et al* (2005). The method combined information from segmented pulmonary vessels and image intensity in the original CT as a means of detection of the fissures to construct a cost image for an airway-guided watershed segmentation. Since the method did not explicitly segment the fissures, the method did not always exactly follow the fissures even when visible in the CT scan. To overcome this, an interactive watershed method was developed to allow for manual correction. Ukil and Reinhardt (2009) utilized information obtained from segmentations of the fissures and airways to come to a lobar segmentation. 3D chest CT scans were processed slice by slice, starting with 2D fissure detection. In cases of incomplete fissures on 2D axial sections, a spline interpolation was used to complete the lobar border guided by information from the airway tree. Manual interaction could be performed in cases where the airway tree did not provide enough information to guide the spline interpolation. Evaluation showed that in 25% of the cases, manual interaction was needed. van Rikxoort *et al* (2010) developed a second lobe segmentation method using the multi-atlas segmentation specifically designed to handle cases with incomplete fissures. As atlases, five cases with complete fissures were selected, and the lung boundaries and fissures were combined into an atlas image for each case. For test cases, the lungs, fissures and bronchi were automatically segmented and combined into a cost image, where information of the bronchi was only taken into account in regions with incomplete fissural information. The most suitable atlas was automatically determined as the atlas that was able to most closely match the fissures to the test image after a fast initial registration and this selected atlas was elastically registered to the test case and the lobar border propagated. The method was evaluated on 20 cases and shown to closely follow the fissures where present. In addition to a specific evaluation on 100 cases with incomplete fissures, an observer rated the quality of the segmentations on a five-point scale, 55 cases got an excellent score for all lobar borders and in 85 cases, all borders were rated as good, only two lobar borders out of 300 were scored as poor. Lassen *et al* (2013) built upon the work of Kuhnigk *et al* (2005) by extending the method to include

information from fissure segmentation and the bronchial tree into the cost image for watershed segmentation. The method was compared to the methods by Kuhnigk *et al* (2005) and van Rikxoort *et al* (2010) on a set of 20 chest CT scans and shown to outperform both.

9.3. Challenges

The segmentation of the pulmonary lobes is one of the most challenging segmentation tasks in the lungs. Radiologists utilize information from the bronchial tree and vasculature when determining the lobar borders in cases with incomplete fissures, but robustly incorporating this information into automated methodology is difficult since the segmentation of the bronchial tree and vasculature are also difficult themselves. Approaches not utilizing this anatomical information might be more robust against segmentation failures, but at the same time are more prone to anatomically incorrect segmentations. A combination of the two strategies might be beneficial.

Most methods were evaluated on a small set of cases, if at all, and usually the scans used were obtained from healthy subjects. As a result, the performance of lobar segmentation methods proposed so far are hard to compare. Lassen *et al* (2013) compared their method to two previously proposed method on a small set of cases but the performance of the other methods cannot be directly compared. In 2011, a grand challenge was organized on lobar segmentation (LOLA11, www.lola11.com) in which only two methods participated (van Rikxoort *et al* 2010, Lassen *et al* 2013). The grand challenge contained a substantial amount of severely diseased cases and showed that both methods were not able to handle these cases successfully, and it is unlikely that other methods proposed so far will. Since the robust automatic segmentation of the lobes in diseased cases needs to be studied and probably is not feasible yet, a method that allows fast interactive correction of lobar segmentation results is desirable. Lassen *et al* (2011) proposed an interactive lobar segmentation method that was submitted to the LOLA11 grand challenge as well and shown to perform very well with minimal user interaction.

Even though the development of automatic lobar segmentation tools is far from finished, their use in clinical research, clinical trials and even clinical practice is growing fast. Many radiologists and pulmonologists are interested in the spread of diseases over the different lobes and its influence on phenotyping and progression of the disease. One example of the use in clinical trials is BLVR treatments with valves. Patient eligibility is determined based on emphysema distribution as well as fissural completeness. In particular, fissural completeness is time consuming to determine for radiologists and given a fissure and lobar segmentation can be automated (Pu *et al* 2010, van Rikxoort *et al* 2012). A large challenge for lobar segmentation for the coming years is to develop methods that perform well and robust in large studies containing scans with pathological abnormalities.

10. Segments

10.1. Relevance

The pulmonary lobes are further subdivided into the pulmonary segments, which have no physical boundaries visible on CT but are defined based on bronchial supply. The pulmonary segments are used by radiologists and pulmonologists to indicate the localization of abnormalities in the lungs and guide interventions. Although the pulmonary segments function less independent within the lung than the lobes, pathological abnormalities might still be confined to a single or several segments, which allows the removal of segments instead of complete lobes. Laros *et al* (1988) performed a 30-year follow-up study of 30 patients in

which ten or more lung segments were removed. The results showed that as long as at least six healthy lung segments were present, the functionality of the lungs did not deteriorate over the course of 30 years. Where the segmentation of the lobes is more and more used, the pulmonary segments are rarely used for the quantification since determining the segmental boundaries is hard and time consuming in 3D CT data. Automated tools might allow for more segmental quantification.

10.2. Methods

In a survey of lung analysis in 2006 (Sluimer *et al* 2006), the automatic segmentation of pulmonary segments was listed as a completely open research area. Since then, the segmentation of the pulmonary segments still received little attention; only two studies are available. The first study is by Kuhnigk *et al* (2005) who, one year before the previous survey, proposed a method to divide the lobes into segments by assigning each voxel in the lobes to the closest branch of an anatomically labeled bronchial tree in the same lobe. The method was evaluated *in vitro* with CT scans of two specimens of the left lungs and showed that 80% of voxels were assigned to the correct lobe, no evaluation was performed for the right lung. A second method was proposed by van Rikxoort *et al* (2009b) as an extension of their lobar segmentation. A voxel classification approach was used using a relative position in the lobe and distance and direction to the fissures as features. The method was trained on manually labeled points of segmental lesions and tested on 100 scans for which two observers manually annotated the segment in which 697 lesions resided. The method performed equally well as the two human observers.

10.3. Challenges

The segmentation of the pulmonary segments remains an open research area. The main difficulty in developing methods for the segmentation of the segments is the reference standard; since there are no physical borders between the segments, obtaining a reference standard on CT data is difficult. Another reason for the little attention for this task is that clinically there does not seem to be an urgent need for the segmentation of the segments at this time.

11. General discussion and conclusion

An automated segmentation of the anatomical structures is a necessary prerequisite for any subsequent analysis of medical imagery. In this review, the automated segmentation of the lungs, vessels, airways, fissures, lobes and segments from thoracic CT scans was discussed. In this general discussion, we attempt to explain the gap between the published literature and the use of segmentation algorithms in clinical practice describes an outlook for the developments in the next years, and draw overall conclusions.

11.1. Evaluation and clinical practice

CT is the most sensitive way to image the lungs *in vivo*. Multi-detector spiral scanning has been available for over 15 years now, and a sizable effort has been made to develop automatic segmentation methods, which is evident from the large number of studies discussed in this review. Most studies report good to excellent results for the segmentation task at hand, often with segmentation results comparable to human experts. In clinical routine, however, almost none of the automatic segmentation tools are used. This gap between clinical practice and

reported results in experimental studies is for a large part due to the variation in chest CT scans obtained in clinical practice compared to the usually small, homogeneous evaluation set of scans used for the evaluation of the performance of segmentation methods. Patient data often contain abnormalities but even healthy, normal anatomy differs widely. Moreover, imaging protocols (as briefly described in section 4) vary between and even within institutions. It is common practice to develop and test methods on data from a single data source, and often the scans used for development and evaluation of segmentation methods are free of disease, or contain only one type of abnormalities. This leads to good results on the evaluation set, but often to disappointing results on other types of data as encountered in clinical routine.

A very important step to bridge the gap between reported results in the literature and experience in clinical practice is quantitative evaluation of the automatic segmentation results on large numbers of scans with different characteristics to ensure that at least the performance is known for each type of scan. However, the quantitative evaluation in 3D chest CT scans is challenging in large cohorts since delineating structures in 3D CT scans in order to construct a standard of reference is time consuming, tedious and tiring for human observers. Several authors opted for evaluating on a subset of slices for which manual segmentations were obtained. Due to the variation in normal anatomy, pathology and other factors, it is preferable to evaluate in a limited set of slices for a large set of scans over completely manually segmenting a small set of cases.

It is not only important to thoroughly evaluate the performance of one specific method, but also to be able to compare the strengths and weaknesses of the different proposed methods. A good opportunity for this is the grand challenges in medical imaging that have been organized since 2007 (www.grand-challenge.org). These grand challenges provide a set of data to apply the methods to, and evaluation is performed centrally, allowing authors to directly compare the results of their method to other methods using the same data and evaluation strategy. For the segmentation of pulmonary structures, grand challenges have been organized for the lungs, vessels, airways and lobes. The grand challenges do not only provide information on which type of methodology might be most suitable for certain tasks, but also reveal that different methods have different strengths and that combining the results of different methods might greatly improve the results (Lo *et al* 2012). The amount of data used in the grand challenges is currently relatively small, mainly since the organizers also need to obtain manual reference standards to allow for evaluation. Repeating the grand challenges by adding data from different sources and with different (pathological) abnormalities to the databases, every couple of years might be a good way to keep evaluating the progress of automated segmentation tasks.

Even in the absence of a grand challenge, it is any way advisable to test algorithms on publicly available data. The publicly available LIDC database, downloadable through the United States National Cancer Institute Imaging Archive web site at http://ncia.nci.nih.gov, provides around 1000 chest CT scans from multiple institutions, in which four radiologists have detected and outlined pulmonary nodules.

11.2. Outlook

Unifying the discussion sections of the different anatomical structures, the following areas appear to be most prominent for future research:

- Employing contextual information
- Automatic error detection
- Interactive tools
- Evaluation on data containing abnormalities.

The different anatomical structures are not always complete or completely visible on chest CT scans, making automated segmentation challenging. However, the structures in the thorax are all related: the position, size and shape of one anatomical structure can provide important clues about the possible positions and shapes of other structures. Since automated segmentation algorithms are available for many anatomical structures in the thorax, it becomes possible to develop methods that combine different segmentations to obtain a reliable segmentation result. Several methods discussed in this review already incorporated contextual information, e.g. Prasad *et al* (2008), Sofka *et al* (2011), Sun *et al* (2012) for the segmentation of lungs, Sonka *et al* (1996), Lo *et al* (2008) for the segmentation of the airways, Bülow *et al* (2005) for the separation of arteries and veins and for the segmentation of the lobes Kuhnigk *et al* (2005), Zhang *et al* (2006), Ukil and Reinhardt (2009), van Rikxoort *et al* (2010), Lassen *et al* (2013). The key to designing such methods is to combine information in a robust and optimal way. The methods proposed so far mainly use the segmentation of auxiliary structures as a given input to enhance the performance of the new segmentation task at hand. In future research, it could be beneficial to attempt to update the segmentation of a set of related structures simultaneously. Another form of contextual information could come from previous scans from the same subject for which segmentations are available, possibly approved or interactively corrected by human experts.

Methods that are able to indicate the probability that the resulting segmentation is correct could be beneficial for the integration of automatic segmentation tools into clinical practice since it might enhance the level of radiologists' trust in the results. An example of automatic error detection for the automatic lung segmentation is provided by van Rikxoort *et al* (2009a), in which a relatively simple error detection method was developed based on statistical deviations from volume and shape measurements of a set of training scans. This error detection was shown to perform well. Although several scans were indicated as possibly containing errors while in reality the results were correct, this is preferable to the reverse situation in which errors are missed. In cases where the method indicates a possible problem with the segmentation and the radiologist confirms this, effective interactive tools should be available to quickly correct the errors. Effective interactive segmentation tools have been proposed for the lungs and lobes (Kockelkorn *et al* 2010a, Lassen *et al* 2011, Sun *et al* 2012) but need to be further developed. Given the high variability in acquisition protocols and pathological abnormalities, it is unlikely that fully automatic segmentation tools will be available in the near future that are able to correctly segment the anatomical structures of interest in every single case. Therefore, for the acceptance of automated analysis into clinical practice, the development of good interactive segmentation tools is vital. An extension to the automatic error detection could not only indicate a possible error but also localize the error and possibly classify into an error category to allow specialized (automatic) methods to locally improve the results.

Finally, methods should be routinely evaluated on rich data sets including scans obtained with different protocols and scans containing abnormalities that range from mild to severe. The data set of the LOLA11 grand challenge is the first to do this for lung and lobe segmentation. In the near future, the amount of publicly available test data is expected to increase rapidly.

11.3. Conclusion

The segmentation is a prerequisite for any automated analysis of lung diseases. Many studies have been reported in the literature, but the completely automatic segmentation of the pulmonary anatomical structures cannot be considered solved yet, although clear improvements have been made over the last decade. The main challenges remain the robustness of segmentation methods on large sets of data, made evident by the recent publications by

Pu *et al* (2012) for lung segmentation, and the performance on cases containing pathological abnormalities. Most methods have been evaluated on small sets of data, usually with no or only mild disease. The grand challenges that have been organized for the segmentation of lungs, airways, vessels and lobes are an important step to be able to compare strengths and weaknesses of different approaches and it would be good to repeat the grand challenges every couple of years by extending the databases of cases with large amounts of new cases to allow continuous monitoring of the progression of the field.

References

Aberle D R, Adams A M, Berg C D, Black W C, Clapp J D, Fagerstrom R M, Gareen I F, Gatsonis C, Marcus P M and Sicks J D 2011 Reduced lung-cancer mortality with low-dose computed tomographic screening *N. Engl. J. Med.* **365** 395–409

Agam G, Armato S G III and Wu C 2005 Vessel tree reconstruction in thoracic CT scans with application to nodule detection *IEEE Trans. Med. Imaging* **24** 486–99

Agarwal M, Hendriks E A, Stoel B C, Bakker M E, Reiber J H C and Staring M 2012 Local SIMPLE multi atlas-based segmentation applied to lung lobe detection on chest CT *Proc. SPIE* **8314** 831410

Ariyürek O M, Gülsün M and Demirkazik F B 2001 Accessory fissures of the lung: evaluation by high-resolution computed tomography *Eur. Radiol.* **11** 2449–53

Armato S G and Sensakovic W F 2004 Automated lung segmentation for thoracic CT: impact on computer-aided diagnosis *Acad. Radiol.* **11** 1011–21

Armato S G *et al* 2004 Lung image database consortium: Developing a resource for the medical imaging research community *Radiology* **232** 739–48

Aykac D, Hoffman E A, McLennan G and Reinhardt J M 2003 Segmentation and analysis of the human airway tree from three-dimensional x-ray CT images *IEEE Trans. Med. Imaging* **22** 940–50

Aziz A, Ashizawa K, Nagaoki K and Hayashi K 2004 High resolution CT anatomy of the pulmonary fissures *J. Thorac. Imaging* **19** 186–91

Boedeker K L, McNitt-Gray M F, Rogers S R, Truong D A, Brown M S, Gjertson D W and Goldin J G 2004 Emphysema: effect of reconstruction algorithm on CT imaging measures *Radiology* **232** 295–301

Brown M S, Goldin J G, McNitt-Gray M F, Greaser L E, Sapra A, Li K T, Sayre J W, Martin K and Aberle D R 2000 Knowledge-based segmentation of thoracic computed tomography images for assessment of split lung function *Med. Phys.* **27** 592–8

Brown M S, McNitt-Gray M F, Mankovich N J, Goldin J G, Hiller J, Wilson L S and Aberle D R 1997 Method for segmenting chest CT image data using an anatomical model: preliminary results *IEEE Trans. Med. Imaging* **16** 828–39

Bülow T, Lorenz C and Renisch S 2004 A general framework for tree segmentation and reconstruction from medical volume data *Int. Conf. on Medical Image Computing and Computer-Assisted Intervention* (*Lect. Notes Comput. Sci.* vol 3216) pp 533–40

Bülow T, Wiemker R, Blaffert T, Lorenz C and Renisch S 2005 Automatic extraction of the pulmonary artery tree from multi-slice CT data *Proc. SPIE* **5746** 730–40

Estépar R S J, Washko G G, Silverman E K, Reilly J J, Kikinis R and Westin C F 2006 Accurate airway wall estimation using phase congruency *Int. Conf. on Medical Image Computing and Computer-Assisted Intervention (Lect. Notes Comput. Sci.* vol 9*)* pp 125–34 PMID: 17354764

Fetita C I, Prêteux F, Beigelman-Aubry C and Grenier P 2004 Pulmonary airways: 3-D reconstruction from multislice CT and clinical investigation *IEEE Trans. Med. Imaging* **23** 1353–64

Frangi A F, Niessen W J, Vincken K L and Viergever M A 1998 Multiscale vessel enhancement filtering *Int. Conf. on Medical Image Computing and Computer-Assisted Intervention (Lect. Notes Comput. Sci* vol 1496*)* pp 130–7

Graham M W, Gibbs J D and Higgins W E 2008 Robust system for human airway tree segmentation *Proc. SPIE* **6914** 69141J

Gu S, Fuhrman C, Meng X, Siegfried J M, Gur D, Leader J K, Sciurba F C and Pu J 2013 Computerized identification of airway wall in CT examinations using a 3D active surface evolution approach *Med. Image Anal.* **17** 283–96

Gu S, Zheng Q, Siegfried J and Pu J 2012 Robust pulmonary lobe segmentation against incomplete fissures *Proc. SPIE* **8315** 831535

Gülsün M, Ariyürek O M, Cömert R B and Karabulut N 2006 Variability of the pulmonary oblique fissures presented by high-resolution computed tomography *Surg. Radiol. Anat.* **28** 293–9

Haussecker H and Jähne B 1996 A tensor approach for local structure analysis in multidimensional images *Proc. 3D Image Analysis and Synthesis* pp 171–8

Hayashi K, Aziz A, Ashizawa K, Hayashi H, Nagaoki K and Otsuji H 2001 Radiographic and CT appearances of the major fissures *Radiographics* **21** 861–74 PMID: 11452059

Hu S, Hoffman E and Reinhardt J 2001 Automatic lung segmentation for accurate quantitation of volumetric x-ray CT images *IEEE Trans. Med. Imaging* **20** 490–8

Jemal A, Bray F, Center M M, Ferlay J, Ward E and Forman D 2011 Global cancer statistics *CA Cancer J. Clin.* **61** 69–90

Kemerink G J, Lamers R J S, Pellis B J, Kruize H H and van Engelshoven J M A 1998 On segmentation of lung parenchyma in quantitative computed tomography of the lung *Med. Phys.* **25** 2432–39

Kim S S, Seo J B, Lee H Y, Nevrekar D V, Forssen A V, Crapo J D, Schroeder J D and Lynch D A 2013 Chronic obstructive pulmonary disease: Lobe-based visual assessment of volumetric CT by using standard images—comparison with quantitative CT and pulmonary function test in the copdgene study *Radiology* **266** 626–35

Kiraly A P, Helferty J P, Hoffman E A, McLennan G and Higgins W E 2004 Three-dimensional path planning for virtual bronchoscopy *IEEE Trans. Med. Imaging* **23** 1365–79

Kockelkorn T T J P, de Jong P A, Gietema H A, Grutters J C, Prokop M and van Ginneken B 2010a Interactive annotation of textures in thoracic CT scans *Proc. SPIE* **7624** 76240

Kockelkorn T T J P, van Rikxoort E M, Grutters J C and van Ginneken B 2010b Interactive lung segmentation in CT scans with severe abnormalities *IEEE Int. Symp. on Biomedical Imaging* pp 564–7

Koller T, Gerig G, Szekely G and Dettwiler D 1995 Multiscale detection of curvilinear structures in 2-D and 3-D image data *Proc. IEEE 5th Int. Conf. on Computer Vision* pp 864–9

Korfiatis P, Kalogeropoulou C, Karahaliou A, Kazantzi A, Skiadopoulos S and Costaridou L 2008 Texture classification-based segmentation of lung affected by interstitial pneumonia in high-resolution CT *Med. Phys.* **35** 5290–302

Korfiatis P D, Kalogeropoulou C, Karahaliou A N, Kazantzi A D and Costaridou L I 2011 Vessel tree segmentation in presence of interstitial lung disease in MDCT *IEEE Trans. Inform. Technol. Biomed.* **15** 214–20

Kuhnigk J M, Dicken V, Bornemann L, Bakai A, Wormanns D, Krass S and Peitgen H O 2006 Morphological segmentation and partial volume analysis for volumetry of solid pulmonary lesions in thoracic CT scans *IEEE Trans. Med. Imaging* **25** 417–34

Kuhnigk J M *et al* 2005 New tools for computer assistance in thoracic CT part 1. Functional analysis of lungs, lung lobes and bronchopulmonary segments *Radiographics* **25** 525–36

Laros C D, van den Bosch J M M, Westermann C J J, Bergstein P G M, Vanderschueren R G J and Knaepen P J 1988 Resection of more than 10 lung segments,a 30-year survey of 30 bronchiectatic patients *J. Thorac. Cardiovasc. Surg.* **95** 119–23

Lassen B, Kuhnigk J M, van Rikxoort E M and Peitgen H O 2011 Interactive lung lobe segmentation and correction in tomographic images *Proc. SPIE* **7963** 79631S

Lassen B, van Rikxoort E M, Schmidt M, Kerkstra S, van Ginneken B and Kuhnigk J 2013 Automatic segmentation of the pulmonary lobes from chest CT scans based on fissures, vessels, and bronchi *IEEE Trans. Med. Imaging* **32** 210–22

Leader J K, Zheng B, Rogers R M, Sciurba F C, Perez A, Chapman B E, Patel S, Fuhrman C R and Gur D 2003 Automated lung segmentation in x-ray computed tomography: development and evaluation of a heuristic threshold-based scheme *Acad. Radiol.* **10** 1224–36

Lesage D, Angelini E D, Bloch I and Funka-Lea G 2009 A review of 3D vessel lumen segmentation techniques: models, features and extraction schemes *Med. Image Anal.* **13** 819–45

Li B, Christensen G E, Hoffman E A, McLennan G and Reinhardt J M 2003 Establishing a normative atlas of the human lung: Intersubject warping and registration of volumetric CT images *Acad. Radiol.* **10** 255–65

Liu X, Primak A N, Yu L, Li H, Krier J D, Lerman L O and McCollough C H 2009 Quantitative evaluation of noise reduction algorithms for very low dose renal CT perfusion imaging *Proc. SPIE* **7258** 72581T

Lo P, Sporring J, Ashraf H, Pedersen J H and de Bruijne M 2008 Vessel-guided airway segmentation based on voxel classification *1st Int. Workshop on Pulmonary Image Analysis (MICCAI)* pp 113–22

Lo P, van Ginneken B and de Bruijne M 2010 Vessel tree extraction using locally optimal paths *IEEE Int. Symp. on Biomedical Imaging* pp 680–3

Lo P *et al* 2012 Extraction of airways from CT (EXACT'09) *IEEE Trans. Med. Imaging* **31** 2093–107

Lozano R *et al* 2012 Global and regional mortality from 235 causes of death for 20 age groups in 1990 and 2010: a systematic analysis for the global burden of disease study 2010 *Lancet* **380** 2095–128

Meng X, Qiang Y, Zhu S, Fuhrman C, Siegfried J M and Pu J 2012 Illustration of the obstacles in computerized lung segmentation using examples *Med. Phys.* **39** 4984–91

Mori K, Hasegawa J, Suenaga Y and Toriwaki J 2000 Automated anatomical labeling of the bronchial branch and its application to the virtual bronchoscopy system *IEEE Trans. Med. Imaging* **19** 103–14

Mori K, Hasegawa J, Toriwaki J, Anno H and Katada K 1996 Recognition of bronchus in three-dimensional x-ray CT images with application to virtualized bronchoscopy system *Int. Conf. on Pattern Recognition* pp 528–32

Nakamura K, Yoshida H, Engelmann R, MacMahon H, Katsuragawa S, Ishida T, Ahizawa K and Doi K 2000 Computerized analysis of the likelihood of malignancy in solitary pulmonary nodules with use of artificial neural networks *Radiology* **214** 823–30 PMID: 10715052

Nimura Y, Kitasaka T, Honma H, Takabatake H, Mori M, Natori H and Mori K 2012 Lung lobe segmentation based on statistical atlas and graph cuts *Proc. SPIE* **8315** 83153B

Ochs R A, Goldin J G, Abtin F, Kim H J, Brown K, Batra P, Roback D, McNitt-Gray M F and Brown M S 2007 Automated classification of lung bronchovascular anatomy in CT using AdaBoost *Med. Image Anal.* **11** 315–24

Odry B L, Kiraly A P, Novak C L, Naidich D P and Lerallut J F 2006 Automated airway evaluation system for multi-slice computed tomography using airway lumen diameter, airway wall thickness and broncho-arterial ratio *Proc. SPIE* **6143** 61430Q

Palágyi K, Tschirren J, Hoffman E A and Sonka M 2006 Quantitative analysis of pulmonary airway tree structures *Comput. Biol. Med.* **36** 974–96

Petersen J, Nielsen M, Lo P, Saghir Z, Dirksen A and de Bruijne M 2011 Optimal graph based segmentation using flow lines with application to airway wall segmentation *Inform. Process. Med. Imaging* **22** 49–60

Prasad M N, Brown M S, Ahmad S, Abtin F, Allen J, da Costa I, Kim H J, McNitt-Gray M F and Goldin J G 2008 Automatic segmentation of lung parenchyma in the presence of diseases based on curvature of ribs *Acad. Radiol.* **15** 1173–80

Prokop M, Galanski M and Schaefer-Prokop C 2003 *Spiral and Multislice Computed Tomography of the Body* (Thieme Medical Publisher) (available at: http://books.google.nl/books?id=K9GbaGpOdGwC)

Pu J, Fuhrman C, Durick J, Leader J K, Klym A, Sciurba F C and Gur D 2010 Computerized assessment of pulmonary fissure integrity using high resolution CT *Med. Phys.* **37** 4661–72

Pu J, Fuhrman C, Good W F, Sciurba F C and Gur D 2011 A differential geometric approach to automated segmentation of human airway tree *IEEE Trans. Med. Imaging* **30** 266–78

Pu J, Gu S, Liu S, Zhu S, Wilson D, Siegfried J M and Gur D 2012 CT based computerized identification and analysis of human airways: a review *Med. Phys.* **39** 2603–16

Pu J, Leader J K, Zheng B, Knollmann F, Fuhrman C, Sciurba F C and Gur D 2009a A computational geometry approach to automated pulmonary fissure segmentation in CT examinations *IEEE Trans. Med. Imaging* **28** 710–9

Pu J, Roos J, Yi C A, Napel S, Rubin G D and Paik D S 2008 Adaptive border marching algorithm: automatic lung segmentation on chest CT images *Comput. Med. Imaging Graph.* **32** 452–62

Pu J, Zheng B, Leader J K, Fuhrman C, Knollmann F, Klym A and Gur D 2009b Pulmonary lobe segmentation in CT examinations using implicit surface fitting *IEEE Trans. Med. Imaging* **28** 1986–96

Raasch B N, Carsky E W, Lane E J, O'Callaghan J P and Heitzman E R 1982 Radiographic anatomy of the interlobar fissures: a study of 100 specimens *Am. J. Roentgenol.* **138** 1043–9

Reinhardt J M, D'Souza N D and Hoffman E A 1997 Accurate measurement of intrathoracic airways *IEEE Trans. Med. Imaging* **16** 820–7

Ross J C, San José Estépar R, Kindlmann G, Díaz A, Westin C F, Silverman E K and Washko G R 2010 Automatic lung lobe segmentation using particles, thin plate splines, and maximum *a posteriori* estimation *Int. Conf. on Medical Image Computing and Computer-Assisted Intervention (Lect. Notes Comput. Sci* vol 13*)* pp 163–71

Saha P K, Gao Z, Alford S K, Sonka M and Hoffman E A 2010 Topomorphologic separation of fused isointensity objects via multiscale opening: separating arteries and veins in 3-D pulmonary CT *IEEE Trans. Med. Imaging* **29** 840–51

Sato Y, Westin C, Bhalerao A, Nakajima S, Shiraga N, Tamura S and Kikinis R 2000 Tissue classification based on 3D local intensity structures for volume rendering *IEEE Trans. Vis. Comput. Graph.* **6** 160–80

Schlathölter T, Lorenz C, Carlsen I C, Renisch S and Deschamps T 2002 Simultaneous segmentation and tree reconstruction of the airways for virtual bronchoscopy *Proc. SPIE* **4684** 103–13

Schmidt M, Kuhnigk J M, Krass S, Owsijewitsch M, de Hoop B and Peitgen H O 2010 Reproducibility of airway wall thickness measurements *Proc. SPIE* **7624** 76241O

Schmidt-Richberg A, Ehrhardt J, Wilms M, Werner R and Handels H 2012 Pulmonary lobe segmentation with level sets *Proc. SPIE* **8314** 83142V

Shamonin D, Staring M, Bakker M, Xiao C, Stolk J, Reiber J and Stoel B 2012 Automatic lung lobe segmentation of COPD patients using iterative B-spline fitting *Proc. SPIE* **8314** 83140W

Shikata H, McLennan G, Hoffman E and Sonka M 2009 Segmentation of pulmonary vascular trees from thoracic 3D CT images *Int. J. Biomed. Imaging* **2009** 636240

Sluimer I, Prokop M and van Ginneken B 2005 Towards automated segmentation of the pathological lung in CT *IEEE Trans. Med. Imaging* **24** 1025–38

Sluimer I C, Schilham A M R, Prokop M and van Ginneken B 2006 Computer analysis of computed tomography scans of the lung: a survey *IEEE Trans. Med. Imaging* **25** 385–405

Sofka M, Wetzl J, Birkbeck N, Zhang J, Kohlberger T, Kaftan J, Declerck J and Zhou S K 2011 Multi-stage learning for robust lung segmentation in challenging CT volumes *Int. Conf. on Medical Image Computing and Computer-Assisted Intervention* vol 14 pp 667–74 PMID: 22003757

Sonka M, Park W and Hoffman E A 1996 Rule-based detection of intrathoracic airway trees *IEEE Trans. Med. Imaging* **15** 314–26

Sun S, Bauer C and Beichel R 2012 Automated 3-D segmentation of lungs with lung cancer in CT data using a novel robust active shape model approach *IEEE Trans. Med. Imaging* **31** 449–60

Sun X, Zhang H and Duan H 2006 3d computerized segmentation of lung volume with computed tomography *Acad. Radiol.* **13** 670–7

Swift R D, Kiraly A P, Sherbondy A J, Austin A L, Hoffman E A, McLennan G and Higgins W E 2002 Automatic axis generation for virtual bronchoscopic assessment of major airway obstructions *Comput. Med. Imaging Graph.* **26** 103–18

Tschirren J, Hoffman E A, McLennan G and Sonka M 2005 Intrathoracic airway trees: segmentation and airway morphology analysis from low-dose CT scans *IEEE Trans. Med. Imaging* **24** 1529–39

Ukil S and Reinhardt J M 2005 Smoothing lung segmentation surfaces in three-dimensional x-ray CT images using anatomic guidance *Acad. Radiol.* **12** 1502–11

Ukil S and Reinhardt J M 2009 Anatomy-guided lung lobe segmentation in x-ray CT images *IEEE Trans. Med. Imaging* **28** 202–14

van Dongen E and van Ginneken B 2010 Automatic segmentation of pulmonary vasculature in thoracic CT scans with local thresholding and airway wall removal *IEEE Int. Symp. on Biomedical Imaging* pp 668–71

van Ginneken B, Baggerman W and van Rikxoort E M 2008 Robust segmentation and anatomical labeling of the airway tree from thoracic CT scans *Int. Conf. on Medical Image Computing and Computer-Assisted Intervention* pp 219–26

van Rikxoort E M, de Hoop B, van de Vorst S, Prokop M and van Ginneken B 2009b Automatic segmentation of pulmonary segments from volumetric chest CT scans *IEEE Trans. Med. Imaging* **28** 621–30

van Rikxoort E M, de Hoop B, Viergever M A, Prokop M and van Ginneken B 2009a Automatic lung segmentation from thoracic computed tomography scans using a hybrid approach with error detection *Med. Phys.* **36** 2934–47

van Rikxoort E M, Goldin J, Abtin F, Kim H J, Lu P, van Ginneken B, Shaw G, Galperin-Aizenberg M and Brown M S 2012 A method for the automatic quantification of the completeness of pulmonary fissures: evaluation in a database of subjects with severe emphysema *Eur. Radiol.* **22** 302–9

van Rikxoort E M, van Ginneken B, Klik M and Prokop M 2008 Supervised enhancement filters: application to fissure detection in chest CT scans *IEEE Trans. Med. Imaging* **27** 1–10

van Rikxoort E M, Prokop M, de Hoop B, Viergever M, Pluim J and van Ginneken B 2010 Automatic segmentation of pulmonary lobes robust against incomplete fissures *IEEE Trans. Med. Imaging* **29** 1286–96

Wang J, Betke M and Ko J P 2006 Pulmonary fissure segmentation on CT *Med. Image Anal.* **10** 530–47

Wang J, Li F and Li Q 2009 Automated segmentation of lungs with severe interstitial lung disease in CT *Med. Phys.* **36** 4592–9

Weinheimer O, Achenbach T, Bletz C, Duber C, Kauczor H U and Heussel C P 2008 About objective 3-d analysis of airway geometry in computerized tomography *IEEE Trans. Med. Imaging* **27** 64–74

Wiemker R, Bülow T and Blaffert T 2005 Unsupervised extraction of the pulmonary interlobar fissures from high resolution thoracic CT data *Int. Cong. Ser.* **1281** 1121–26

Wittenberg R, Peters J F, Weber M, Lely R J, Cobben L P J, Prokop M and Schaefer-Prokop C M 2012 Stand-alone performance of a computer-assisted detection prototype for detection of acute pulmonary embolism: a multi-institutional comparison *Br. J. Radiol.* **85** 758–64

Xiao C, Staring M, Shamonin D, Reiber J H C, Stolk J and Stoel B C 2011 A strain energy filter for 3d vessel enhancement with application to pulmonary CT images *Med. Image Anal.* **15** 112–24

Zhang L, Hoffman E A and Reinhardt J M 2006 Atlas-driven lung lobe segmentation in volumetric x-ray CT images *IEEE Trans. Med. Imaging* **25** 1–16

Zhou C, Chan H P, Kuriakose J W, Chughtai A, Wei J, Hadjiiski L M, Guo Y, Patel S and Kazerooni E A 2012 Pulmonary vessel segmentation utilizing curved planar reformation and optimal path finding (CROP) in computed tomographic pulmonary angiography (CTPA) for CAD applications *Proc. SPIE* **8315** 83150N

Zhou C, Chan H P, Sahiner B, Hadjiiski L M, Chughtai A, Patel S, Wei J, Ge J, Cascade P N and Kazerooni E A 2007 Automatic multiscale enhancement and segmentation of pulmonary vessels in CT pulmonary angiography images for CAD applications *Med. Phys.* **34** 4567–77